Accepted Manuscript

Design, synthesis, and evaluation of isoflavone analogs as multifunctional agents for the treatment of Alzheimer's disease

Dongmei Wang, Min Hu, Xinpeng Li, Dan Zhang, Chengjuan Chen, Junmin Fu, Shuai Shao, Gaona Shi, Yu Zhou, Song Wu, Tiantai Zhang

PII: S0223-5234(19)30167-9

DOI: https://doi.org/10.1016/j.ejmech.2019.02.053

Reference: EJMECH 11145

To appear in: *European Journal of Medicinal Chemistry*

Received Date: 29 December 2018

Revised Date: 14 February 2019

Accepted Date: 17 February 2019

Please cite this article as: D. Wang, M. Hu, X. Li, D. Zhang, C. Chen, J. Fu, S. Shao, G. Shi, Y. Zhou, S. Wu, T. Zhang, Design, synthesis, and evaluation of isoflavone analogs as multifunctional agents for the treatment of Alzheimer's disease, *European Journal of Medicinal Chemistry* (2019), doi: https://doi.org/10.1016/j.ejmech.2019.02.053.

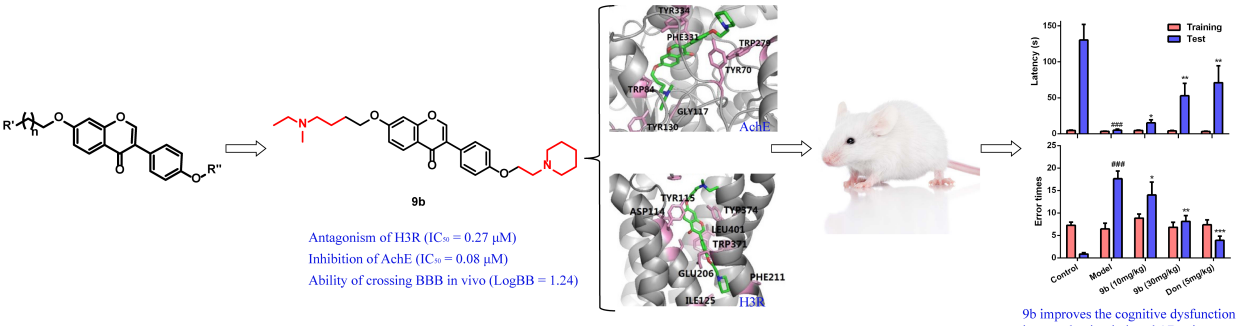

Design, synthesis, and evaluation of isoflavone analogs as multifunctional agents for the treatment of Alzheimer's disease

Dongmei Wang[a,1], Min Hu[a,1], Xinpeng Li[b], Dan Zhang[c], Chengjuan Chen[a], Junmin Fu[a], Shuai Shao[a], Gaona Shi[a], Yu Zhou[a], Song Wu[a,**], Tiantai Zhang[a,*]

[a] *State Key Laboratory of Bioactive Substance and Function of Natural Medicines, Institute of Materia Medica, Chinese Academy of Medical Sciences and Peking Union Medical College, Beijing 100050, China;*
[b] *Food and Drug Administration of Beijing Yanqing District, Beijing 102100, China*
[c] *Department of Pharmacy, China-Japan Friendship Hospital, Beijing 100029, China*

[*] **Corresponding author.** State Key Laboratory of Bioactive Substance and Function of Natural Medicines, Institute of Materia Medica, Chinese Academy of Medical Sciences and Peking Union Medical College, Beijing 100050, China.

[**] **Corresponding author.** State Key Laboratory of Bioactive Substance and Function of Natural Medicines, Institute of Materia Medica, Chinese Academy of Medical Sciences and Peking Union Medical College, Beijing 100050, China.

E-mail address: ttzhang@imm.ac.cn (Tiantai Zhang); ws@imm.ac.cn (Song Wu).

[1] These authors contributed equally to this work.

Abstract

A series of novel isoflavone analogs were designed, synthesized, and evaluated as multitarget-directed ligands for the treatment of Alzheimer's disease. *In vitro* evaluations revealed that some ligands had multifunctional profiles, including potent blockage of histamine 3 receptor (H3R), excellent inhibition of acetylcholinesterase (AChE), neuroprotective effects and anti-neuroinflammatory properties. Among these derivatives, compound **9b** exhibited the highest ability to block H3R (IC_{50} = 0.27 μM) and good inhibitory activity against AChE (IC_{50} = 0.08 μM). Additionally, compound **9b** showed obvious neuroprotective effect on SH-SY5Y by preventing copper-induced neuronal damage and potent anti-neuroinflammatory activity by inhibiting the production of inflammatory factors on BV-2 cells. A molecular modeling study revealed that **9b** acts as a mixed-type inhibitor that interacts simultaneously with H3R and AChE. Moreover, *in vivo* data revealed that compound **9b** did not cause acute toxicity in mice at doses up to 1000 mg/kg, and had desirable pharmacokinetic properties, as well as a good blood-brain barrier (BBB) permeability (log BB = 1.24 ± 0.07). Further studies demonstrated that chronic oral treatment with **9b** significantly improved cognitive dysfunction in scopolamine-induced AD mice in the step-down passive avoidance test. Taken together, the present study showed that compound **9b** is a promising multifunctional drug candidate for the treatment of Alzheimer's disease.

Key words: Alzheimer's disease; isoflavone analogs; histamine 3 receptor; acetylcholinesterase; neuroprotection; multifunctional agents

1. Introduction

Alzheimer's disease (AD) is the most common cause of dementia, and is characterized by progressive memory loss and cognitive impairment. It affects more than 24 million people worldwide, with an increasing trend in case numbers [1]. Although the exact etiology of AD is not fully known, there are diverse factors that seem to play vital roles in the pathophysiology of the disease, including neuron loss, β-amyloid (Aβ) deposits, tau protein hyperphosphorylation, metal ion dyshomeostasis,

oxidative stress, neuroinflammation, and neurotransmitter system dysfunction [2-4]. Since the pathogenesis of AD is complicated, and multiple factors are involved in the pathological process of AD, the underlying mechanism of AD progression remains unclear and there is no current effective treatment for the disease. To date, there are only four acetylcholinesterase (AChE) inhibitors and one N-methyl-D-aspartate (NMDA) receptor antagonists approved to treat AD by the US Food and Drug Administration (FDA). These drugs can improve the cognitive function symptoms, but fail to reverse or delay the progression of AD.

Considering the complex pathogenesis of AD, multifunctional agents that simultaneously interfere with two or more pathogenic AD factors might be good candidates for treating AD. Thus, multitarget-directed ligands (MTDLs) that take into account multiple biological factors of AD are a new strategy in the drug discovery for AD [5, 6]. Based on this strategy, a number MTDLs were developed by modifying commercial drugs or optimizing structure of natural product to simultaneously modulate multi-targets and exert multiple beneficial activities against AD [7-9]. Among targets related to AD, AChE is considered as a primary target. It could be combined with other targets to design and synthesis of MTDLs, such as AChE combining with BuChE [10], AChE combing with BACE1 [11], AChE combing with calcium channel [7], AChE combing with Monoamine oxidase [8].

Histamine and acetylcholine (ACh) are important neurotransmitters in the central nervous system (CNS) that are associated with memory and cognitive function in AD through the histamine 3 receptor (H3R) and AChE, respectively [12, 13]. H3Rs are primarily found in the CNS, and mainly expressed in the globus pallidus, basal ganglia, hippocampus and cortex [14]. It controls the synthesis and release of histamine and other neurotransmitters including ACh, dopamine, glutamate, serotonin, γ-aminobutyric acid and norepinephrine [15]. Constitutive H3R activation leads an inhibition of neurotransmitter release and influences brain disorders like AD, schizophrenia and epilepsy. Selective H3R antagonists such as ABT238, GSK-239512 and MK-3134 (Fig.1), have been linked to increases in cognition and spatial memory in numerous animal experiments. Currently, four single-targeted AChE inhibitors

(donepezil, tacrine, rivastigmine, and galantamine) are the main clinical drugs for the treating AD.

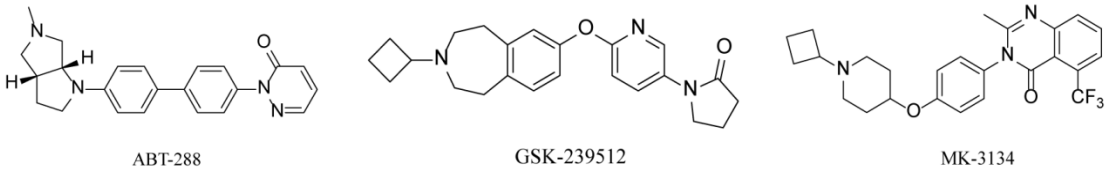

Fig. 1. Structures of H3R antagonists in clinical trials.

Increasing evidences indicate that neuronal injury and neuroinflammation play important roles in the progression of AD [16, 17]. Neuroprotection and anti-neuroinflammation are also valuable tools to slow down the progression of AD. Therefore, the successful protection of neuronal cells from damage and inhibiting inflammatory response of microglial cells may potentially prevent the development of AD. Consequently, strategies such as simultaneously targeting H3R and AChE, protecting neuronal cells from damage, inhibiting the inflammatory response of the nervous system have been envisaged for AD treatment.

Our previous studies have shown that isoflavone analogs exhibit cholinesterase inhibitory activity [18, 19]. Inspired by these discoveries, we aimed to create a new family of MTDL molecules that can inhibit AChE activity, block H3R, or possess other biological activities. More than twenty compounds [18, 19] with inhibitory activity towards AChE were selected to evaluate their antagonistic activity on H3R. Encouragingly, four compounds (**A**, **B**, **C**, and **D**, Table 1) showed simultaneous antagonistic activity on H3R. Preliminary structure-activity relationship (SAR) analysis indicated that the introduction of piperidine or *N*-ethyl-*N*-methyl-alkylamine at the 7-position generates good H3R antagonist activity (compound **A**, **B**, or **D**). The four-carbon chain between the amino group and isoflavone core seems to be better than three-carbon chain (compound **B** vs **D**). However, the introduction of *N*-ethyl-*N*-methyl-alkylamine at the 7-position seems to reduce the inhibitory activity of BuChE. In addition, the di-substitution at the 7, 4'-position of isoflavone appears to

be helpful for exerting multitarget inhibitory activities (compound **C**). These findings could aid us to develop new promising multifunctional agents that target H3R, and AChE, and possess other activities, such as neuroprotection, anti-neuroinflammation, and so on.

We did the rationale design following these four points. Firstly, different amine groups were introduced to the 7-position of isoflavone core beyond piperidine or *N*-ethyl-*N*-methyl-alkylamine, for example, primary amines, secondary amines, or amide, to test the effect on the activities. Secondly, in order to find optimal linker between the amino group and isoflavone core, we designed two- or four-carbon chain or changed alkyl to alkoxy chain. Thirdly, tacrine, a good AChE and BuChE inhibitor, was introduced into the 7-position of isoflavones to evaluate whether it contributed to the multitarget inhibition activity. Besides, one of the important H3R antagonists reported in the literature is the diamine-based ligand [20-22]. Those diamie-based antagonists contain an aromatic ring and two basic functional groups flanking a lipophilic core. Encouraged by the results and our discoveries, we reasoned that incorporation of the isoflavone scaffold with the diamine groups could furnish a viable platform for the development of H3R, AChE, and other functional effects.

In the current study, we have reported on the design, synthesis and biological evaluation of 11 new isoflavone analogs (**2a-9c**) based on our previous developments. After evaluating all compounds for the inhibition of ChE (including AChE and BuChE) and antagonistic activity towards H3R, the outstanding compound, **9b**, was selected for further evaluation. We investigated its neuroprotective effects *in vitro*, anti-neuroinflammatory effects, *in vivo* acute toxicity effects and pharmacokinetic profile, including BBB permeability and cognitive function. The ability of **9b** to cross the BBB was also predicted *in silico* by the "ADMET Descriptors" module implemented in DS2016. Furthermore, molecular modeling studies were performed to investigate the binding mode and the structure-activity relationships of **9b** with targets.

Table 1. The results of first-round screening.

Comp.	Chemical structures	IC_{50} (μM)[a]		
		H3R	AChE[b]	BuChE[c]
A	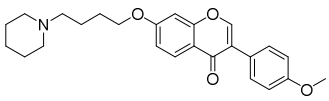	0.73±0.01	3.98±0.02	8.83±0.02
B	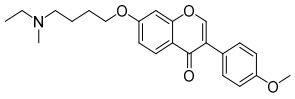	0.43±0.002	9.47±0.04	n.a.[d]
C	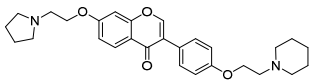	2.07±0.01	0.71±0.02	4.55±0.02
D	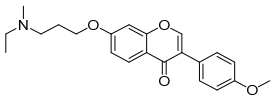	0.52±0.008	22.60±0.05	n.a.[d]

[a] IC_{50} values represent the concentration of inhibitor required to decrease enzyme activity or H3R activity by 50% and are the mean of three independent experiments, each performed in triplicate (SD = standard deviation).

[b] AChE was extracted from mouse brains.

[c] BuChE was derived from mouse plasma.

[d] n.a.= no active. Compounds defined "no active" means a percent inhibition of less than 5.0% at a concentration of 10 μM in the assay conditions.

2. Results and discussion

2.1. Chemistry

The synthetic route of the new isoflavone analogs is depicted in Schemes 1 and 2. The bromo-substituted intermediates **1a** and **1b** were prepared using commercially available formononetin and dibromodiethyl ether in acetone in the presence of potassium carbonate. Thereafter, with various amine intermediates available, target molecules of **2a-2e** were synthesized in the presence of potassium carbonate [19]. In addition, compound **3** was obtained by removal of tert-butoxycarbonyl groups from compound **2e** in the presence of hydrochloric acid. Compound **6** was obtained by reaction of compound **3** with 9-chloro-1,2,3,4-tetrahydroacridine in the presence of phenol and sodium iodide. The synthesis of starting materials **A**, **B**, and **E** shown in Scheme 2 has been reported previously by our team [18]. The demethylation of **A, B,** and **E** in the presence of 40% hydrobromic acid provided compounds **7a-7c**, which

were then reacted with 1,2-dibromoethane in acetone in the presence of potassium carbonate to produce **8a**-**8c**. Finally, reaction of **8a**-**8c** with piperidine produced the target compounds **9a**-**9c**. The structures of all target compounds were confirmed by high-resolution mass spectroscopy (HRMS) and ^{1}H and ^{13}C nuclear magnetic resonance (NMR) spectroscopy.

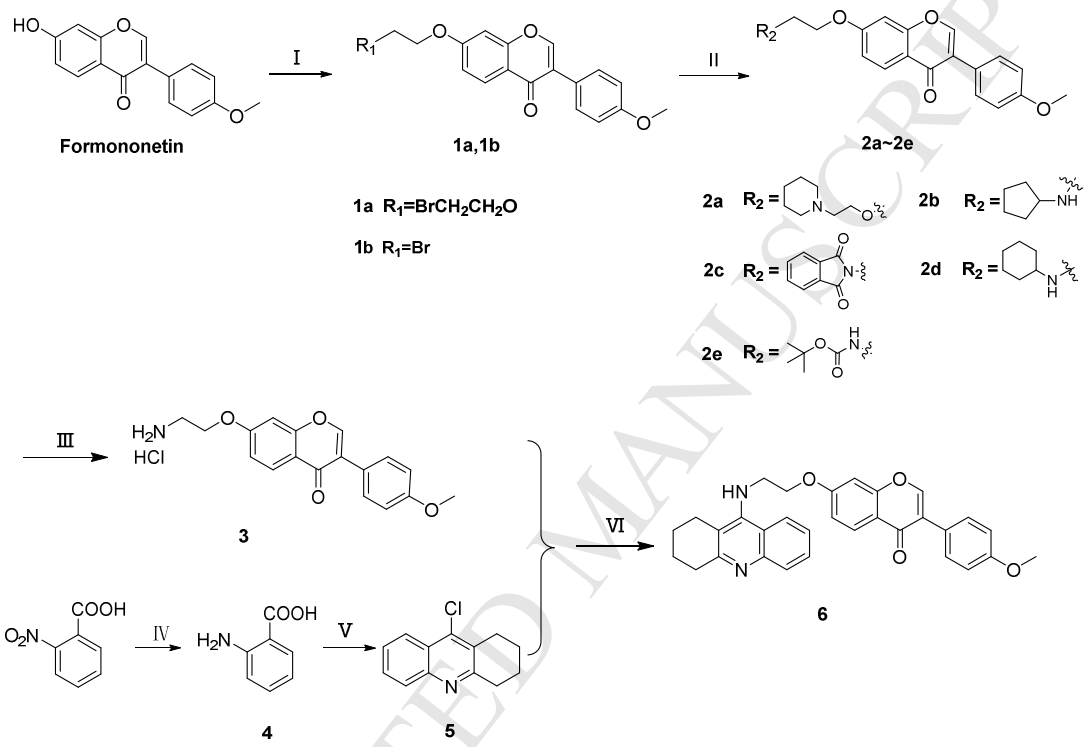

Scheme 1. The synthesis of target compounds **2a-2e**, **3**, and **6**. Reagents and conditions: (I) K_2CO_3, acetone, $Br(CH_2)_2Br$ or $Br(CH_2)_2O(CH_2)_2Br$, 60°C; (II) amines, K_2CO_3, DMF/acetonitrile, 100°C, 3 h; (III) 30-40% HCl/EtOH, RT, 20 min (from **2e**); (IV) Pd/C, H_2, CH_3OH, RT, 8 h; (V) $POCl_3$, cyclohexanone, refluxing, 1 h; (VI) NaI, PhOH, Ar_2, 180°C, 2 h.

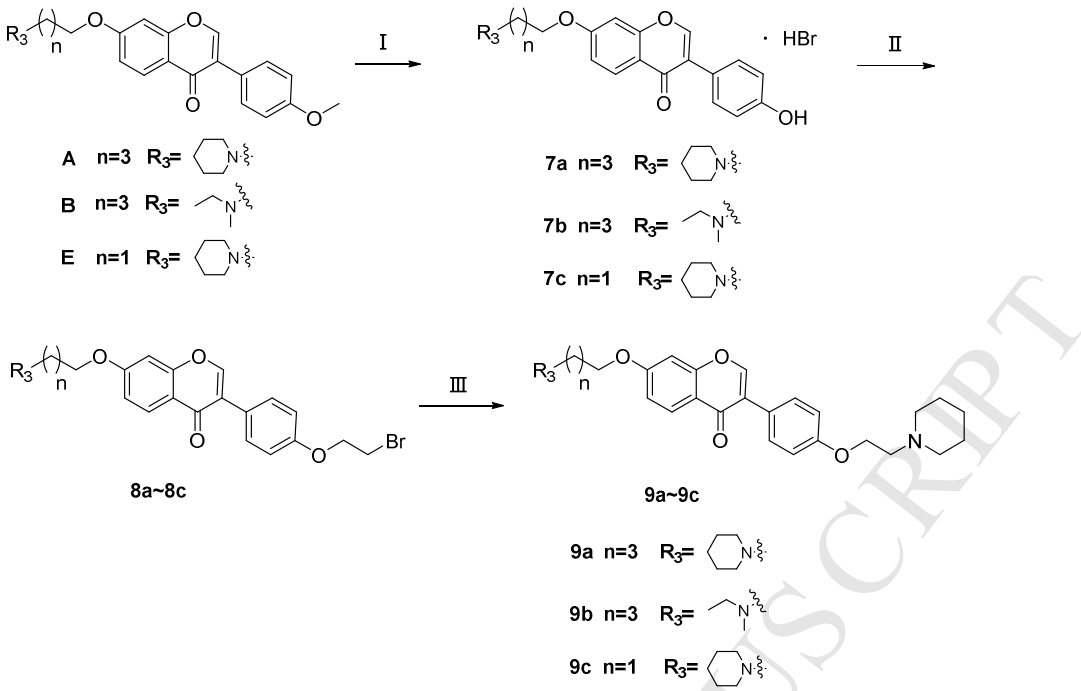

Scheme 2. The synthesis of target compounds **7a** and **9a-9c**. Reagents and conditions: (I) 40% HBr, 120°C, 3 h; (II) K_2CO_3, acetone, $Br(CH_2)_2Br$, 60°C; (III) piperidine, acetonitrile.

2.2. Inhibition of the histamine H3R

Compounds **2a-9c** were evaluated for H3R antagonistic activity by analyzing U2OS cells stably expressing human recombinant H3R with a LiveBLAzer FRET-B/G loading Kit (Invitrogen, USA). The H3R antagonist thioperamide was used as a positive control agent. The antagonistic potencies of tested compounds are presented in Table 2. It was clear that compounds **9a-9c** showed antagonistic activity, with IC_{50} values of 0.41, 0.27 and 1.94 μM, respectively. The IC_{50} values were compared with the thioperamide as a positive control agent. The SAR study indicated that *N*-ethyl-*N*-methyl-alkylamine at the 7-position of isoflavone exhibited apparent higher H3R antagonistic activity than piperidine substitution (compound **B** vs **A**; compound **9b** vs **9a**). Regarding the linker length between the amino group and isoflavone core, the optimal carbon number seems to be four (compound **B** vs **D**). In addition, the di-substitution at the 7,4'-position led to a clearly increase in activity; when compared to corresponding mono-substituted compounds (compounds **9a** vs **A**; **9a** vs **7a**; **9b** vs **B**).

Table 2 Biological evaluation of the inhibitory activity of **2a-2e**, **3, 6, 7a,** and **9a-9c** against H3R, AChE, and BuChE activity.

Comp.	Inhibition (%) at 10 μM[a]			IC_{50} (μM)[b]		
	H3R	AChE[c]	BuChE[d]	H3R	AChE[c]	BuChE[d]
2a	30.32	35.03	12.41	>50	>50	>50
2b	47.12	78.49	80.31	>50	4.50±0.02	5.98±0.01
2c	-15.63	11.19	-9.87	n.a.[e]	>50	n.a.[e]
2d	41.02	73.71	66.00	>50	5.00±0.03	21.59±0.12
2e	-197.9	-0.17	0.12	n.a.[e]	n.a.[e]	n.a.[e]
3	-6.69	16.95	4.82	n.a.[e]	>50	n.a.[e]
6	60.49	85.80	97.12	>10	0.96±0.01	0.38±0.01
7a	6.88	63.38	50.25	>50	26.79±0.14	24.77±0.11
9a	72.36	85.07	86.37	0.41±0.01	0.20±0.003	2.49±0.01
9b	75.24	92.75	81.30	0.27±0.004	0.081±0.0002	2.89±0.02
9c	71.45	82.79	91.55	1.94±0.01	0.35±0.01	2.92±0.01
Thioperamide	71.12	NT[f]	NT[f]	1.03±0.01	NT[f]	NT[f]
Donepezil	NT[f]	88.99	NT[f]	NT[f]	0.084±0.0003	NT[f]
Rivastigmine	NT[f]	NT[f]	93.15	NT[f]	NT[f]	0.058±0.001

[a] Data are presented as the mean of three independent experiments

[b] IC_{50} values represent the concentration of inhibitor required to decrease enzyme activity or H3R activity by 50% and are the mean of three independent experiments, each performed in triplicate (SD = standard deviation).

[c] AChE was extracted from mouse brains.

[d] BuChE was derived from mouse plasma.

[e] n.a.= no active. Compounds defined "no active" means a percent inhibition of less than 5.0% at a concentration of 10 μM in the assay conditions.

[f] NT = not tested.

2.3. Cholinesterase (ChE) inhibitory activity

The cholinesterase inhibitory activities of compounds **2a-9c** were determined using Ellman's assay on AChE and BuChE [23]. The well-known ChE inhibitors Donepezil and rivastigmine were selected as reference compounds of AChE and BuChE,

respectively. The results are summarized as IC_{50} value and percentage of inhibition at 10 μM in Table 2.

The data in Table 2 indicates that the activity decreased to almost zero after the alkyl chain between the amino group and isoflavone core of compound **A** was substituted with the same length of alkoxy chain (**2a**). This indicates that the alkyl chain is essential for the retention of inhibitory activity. The optimal carbon number between the amino group and isoflavone core seems to be four (compound **B** vs **D**; **9a** vs **9c**).

In addition, the terminal groups NR_1R_2 of the side chain exerted significant effects on ChE inhibitory activities. Several amine-containing compounds, including secondary amines and amide were introduced to formononetin (**2a, 2b, 2c, 2d, 2e, 3** and **6**) to optimize ChE inhibitory activities. The results show most compounds decrease in activity in comparison with compound **A** which contains the piperidine group. As expected, compound **6**, bearing 9-amino-1,2,3,4-tetrahydroacridine, exhibited more potent inhibition of AChE (IC_{50} = 0.96 μM) and BuChE (IC_{50} = 0.38 μM) than compound **A**. 9-amino-1,2,3,4-tetrahydroacridine, known as Tacrine, is an FDA-approved acylcholinesterase inhibitor that is clinically used to treat AD (now discontinued). *N*-ethyl-*N*-methyl-alkylamine at the 7-position of isoflavone exhibited apparent higher AChE antagonistic activity than piperidine substitution (compound **B** vs **A**; **9b** vs **9a**).

Three bi-substituted compounds (**9a-9c**) were synthesized. Encouragingly, these compounds exhibited pronounced dual-inhibitory effects on AChE and BuChE activity, and their inhibitory activities were very similar at the micromolar level. Compound **9b** exhibited the highest inhibitory activity on AChE (IC_{50} = 0.081 μM), with moderate inhibitory activity on BuChE (IC_{50} = 2.89 μM). The inhibitory activity of **9b** on AChE was equivalent to the positive control donepezil (0.084 μM). Those results also confirmed that the di-substitution at the 7, 4'-position contributed to the increase in ChE inhibitory activity compared to corresponding mono-substituted compounds.

2.4. Antioxidant activity

Oxidative stress can induce cellular damage and promote neurodegenerative diseases [24]. Antioxidant activity is therefore beneficial for AD treatment. The antioxidant activities of compounds were evaluated by the oxygen radical absorbance capacity assay method using fluorescein (ORAC-FL) [25, 26]; the vitamin E analogue trolox was used as a standard. All the isoflavone analogs exhibited potent peroxyl radical absorbance capacities, ranging from 0.01 to 0.88 trolox equivalents, as shown in Table 3. Most compounds presented moderate antioxidant activity, with an activity of 0.11 trolox equivalents.

Table 3 Antioxidant activity of isoflavone analogs **A-D**, **2a**-**2e**, **3**, **6**, **7a**, and **9a**-**9c**.

Comp.	Trolox equivalent[a]	Comp.	Trolox equivalent[a]
A	0.07±0.001	**2e**	0.05±0.001
B	0.11±0.002	**3**	0.08±0.001
C	0.14±0.002	**6**	0.01±0.0003
D	0.12±0.003	**7a**	0.88±0.003
2a	0.01±0.0001	**9a**	0.11±0.002
2b	0.01±0.0002	**9b**	0.01±0.0001
2c	0.01±0.0004	**9c**	0.14±0.004
2d	0.01±0.0004	**Trolox**	1±0.0001

[a] Results are expressed as μM of Trolox equivalent/μM of tested compound and data are presented as the mean ± SD of three independent experiments.

2.5. Molecular modeling studies

To further elucidate the binding interactions between compound **9b** and AChE or H3R, a molecular modeling study was performed using the Gold 3.0.1 software package [27]. AChE (PDB: 1EVE) or homology model of H3R in complex with compound **9b** were pretreated by the Discovery Studio program (BIOVIA Inc, San Diego, CA). The Discovery Studio 2016 and PyMol programs were used to display 2D and 3D models from the molecular docking and show the different interaction

types between compound **9b** and AChE or H3R.

Figures 2 and 3 shows compound **9b** localizes in the long tunnel of the active site, which occurs through intermolecular hydrophobic and hydrophilic interactions. Our studies showed compound **9b** bonds to key amino acid residues Tyr70 and Gly117 via hydrogen bonding. The aromatic ring structure of compound **9b** also displays π-π overlap interactions with Tyr34 and Phe331 in the catalytic cleft. Significantly, Trp279 was found to bind to the nitrogen atoms on the piperazine group of compound **9b** by π-cation interactions. These results show compelling evidence that compound **9b** can stably combine with AChE (Fig. 2).

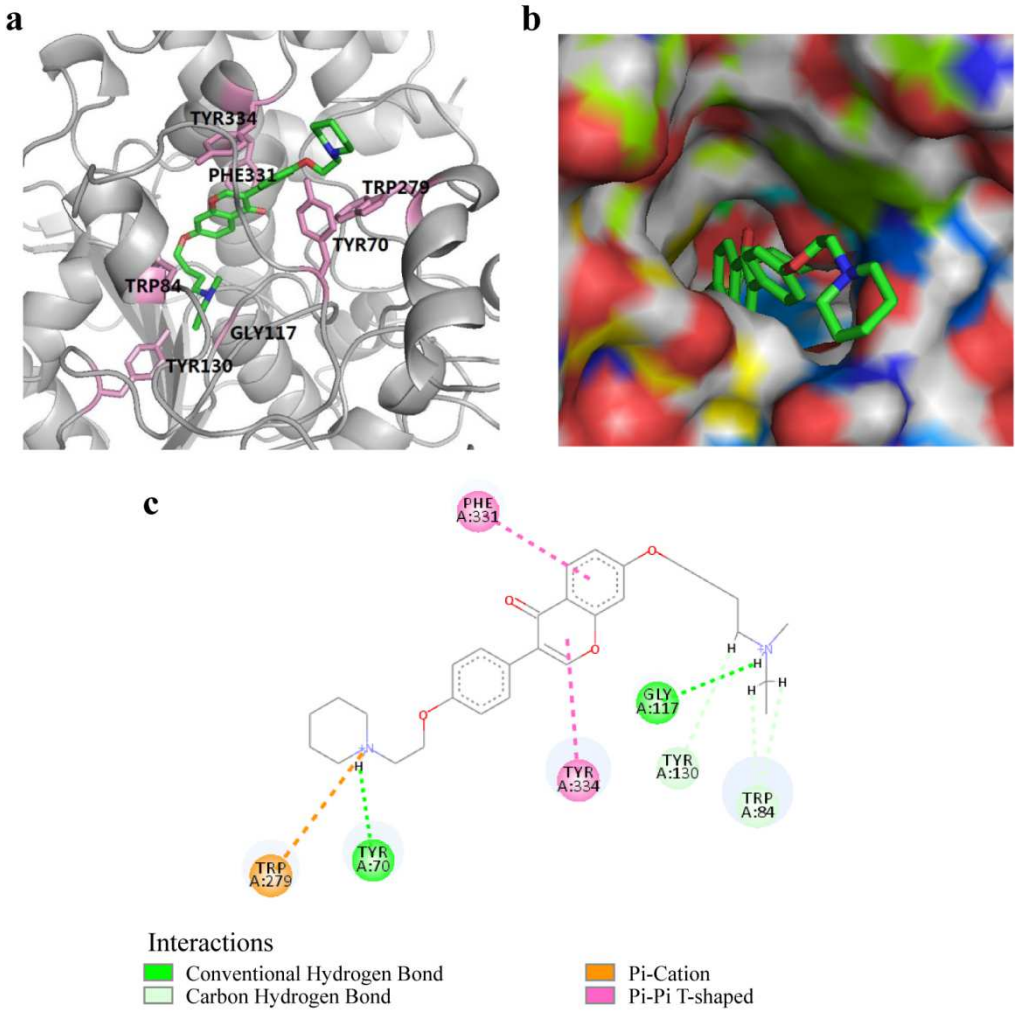

Fig. 2. (**a**) The predicted binding mode of compound **9b** with AChE; (**b**) the binding pocket of AChE by the surface representation; (**c**) 2D schematic diagram of potential interactions between compound **9b** and AChE.

The homology model of H3R was built based on the crystal structure of the human histamine 1 receptor (PDB:3RZE) in complex with the doxepin antagonist [19]. As shown in Fig. 3, the isoflavone core structure of small molecule ligands bind to Trp371, Tyr115, and Tyr374 by π-π interaction. Additionally, a salt bridge with Glu206 also contributes to the stabilization of protein–ligand interaction. Again, these interactions contribute to small molecule ligands adopting the appropriate orientation to bind effectively to the active site.

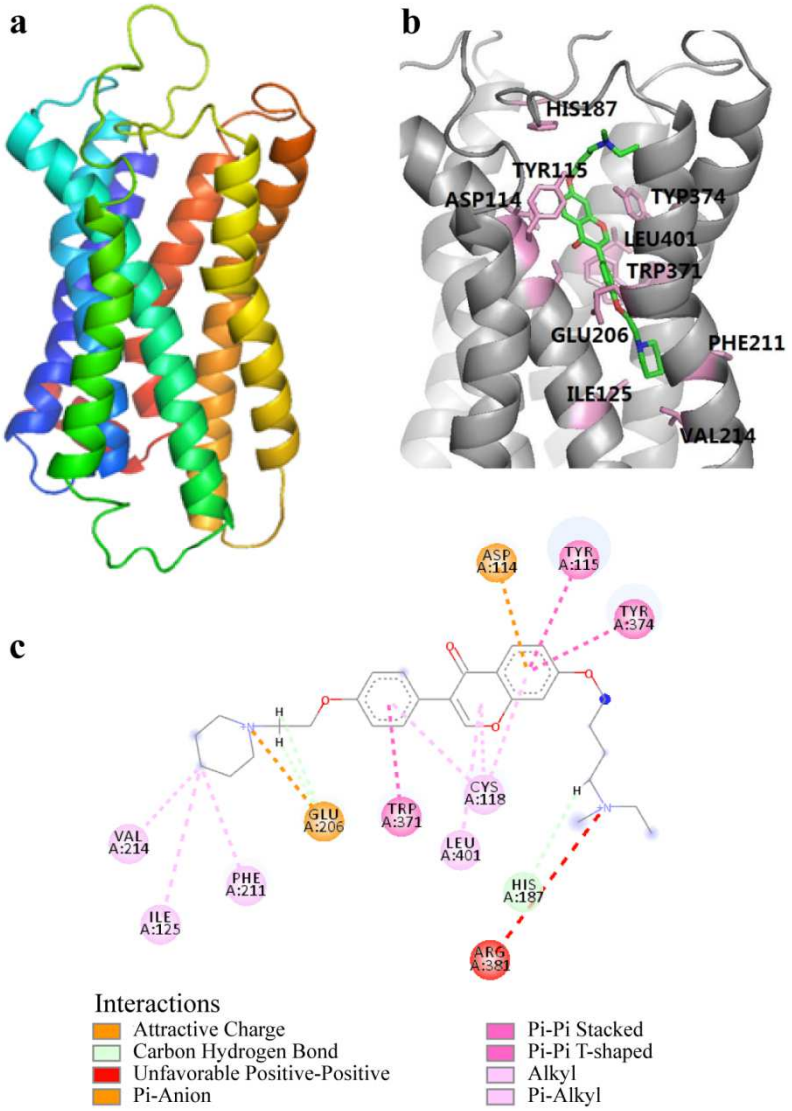

Fig. 3. (**a**) The best homology model of H3R generated by DS MODELER; (**b**) the binding pocket of H3R by surface representation; (**c**) 2D schematic diagram of potential interactions between compound **9b** and H3R.

2.6. ADMET in silico prediction

As shown in Table 4, all compounds appeared to have very poor solubility in aqueous media and have high hydrophobicity, whereas they possessed adequate absorption except compound **6**. Fortunately, three compounds with greater inhibitory activity (**9a-9c**) were predicted to penetrate the BBB, which is a desirable property for the treatment of AD. These compounds also may not bind to CYP2D6, which is beneficial for ensuring therapeutic efficacy and avoiding side effects. In this prediction, however, most compounds exhibit hepatotoxicity, therefore further biological experiments are required to obtain additional data for testing this.

Table 4 Predicted pharmacokinetic properties of isoflavone analogs **A~D**, **2a-2e**, **3**, **6**, **7a**, and **9a-9c.**

Comp.	AlogP98.	PSA-2D	Solubility Level	Absorption Level	BBB Level	PPB	CYP2D6	Hepatotoxic
A	4.532	47.443	2	0	1	true	true	false
B	3.963	47.443	2	0	1	true	true	true
C	3.433	47.443	2	0	1	true	true	true
D	3.889	47.443	2	0	1	true	true	true
2a	3.758	56.373	2	0	1	false	true	false
2b	3.838	56.901	2	0	1	true	true	true
2d	4.295	56.901	2	0	1	true	true	true
2c	4.039	82.045	2	0	2	true	false	true
2e	3.6	83.132	2	0	2	true	false	true
3	2.004	70.631	3	0	3	true	false	true
6	5.997	68.162	1	1	4	true	false	true
7a	4.306	59.328	2	0	1	true	true	false
9a	5.588	50.796	2	0	0	true	false	true
9b	5.019	50.796	2	0	1	true	false	true
9c	4.945	50.796	2	0	1	true	false	true

AlogP98: Lipophilicity descriptor.
PSA-2D: Polar surface area.
Solubility Level: (0, good; 1, moderate; 2, poor; 3, very poor).
Absorption Level: (0, good; 1, moderate; 2, poor; 3, very poor).
BBB Level: (0, very high blood–brain barrier penetration; 1, high; 2, medium; 3, low).
PPB Prediction: The classification describing whether a compound is highly bound (>= 90% bound) to plasma proteins using the cutoff Bayesian score of -2.209 (obtained by minimizing the total number of false positives and false negatives).
CYP2D6 Prediction: The classification describing whether a compound is a CYP2D6 inhibitor using the cutoff Bayesian score of 0.161 (obtained by minimizing the total number of false positives and false negatives).
Hepatotoxic Prediction: The classification describing whether a compound is hepatotoxic using the cutoff Bayesian score of -4.154 (obtained by minimizing the total number of false positives and false negatives).

*2.7. Cytotoxicity and neuroprotective effects of **9b***

Cytotoxic activity of the **9b** was tested using human neuroblastoma cells, SH-SY5Y. The results showed that 9b has a low cytotoxicity (CC_{50} > 100 μM) and high antagonism effect for H3R (IC_{50} = 0.27μM), inhibition activity for AChE (IC_{50} = 0.081μM) and BuChE (IC_{50} =2.89 μM), resulting in a high selectivity index (SI, CC_{50}/IC_{50}) of > 370.37, > 1234.56 and > 34.6, respectively (Table 5).

Table 5 *In vitro* cytotoxicity, H3R antagonism activity, AChE and BuChE inhibitory activity and selectivity index of compound **9b**.

Comp.	SH-SY5Y	H3R		AChE		BuChE	
	CC_{50} (μM)[a]	IC_{50} (μM)[b]	SI[c]	IC_{50} (μM)	SI	IC_{50} (μM)	SI
9b	>100	0.27±0.004	>370.37	0.081±0.0002	>1234.56	2.89±0.02	>34.6
Thioperamide	85.79±0.9	1.03±0.01	83.29	NT[d]	-	NT	-
Donepezil	25.06±0.4	NT	-	0.084±0.0003	298.33	NT	-
Rivastigmine	67.82±0.7	NT	-	NT	-	0.058±0.001	1169.3

[a] CC_{50} 50% cytotoxic concentrations, values represented as average of at least triplicate measurements (mean ± SD).

[b] IC_{50} 50% inhibitory concentration, values represent the concentration of inhibitor required to decrease enzyme activity or H3R activity by 50% and are the mean of three independent experiments, each performed in triplicate (mean ± SD).

[c] SI (selectivity index) = CC_{50}/IC_{50}.

[d] NT = not tested.

To further assess the therapeutic potential of **9b** for AD, the neuroprotective activity of **9b** was assessed by measuring copper induced cell viability against SH-SY5Y-APPsw cell line, which is a useful AD model by overexpresses the Swedish mutant form of human APP [17]. As shown in Fig. 4a, **9b** did not affect cell viability up to the concentration of 100 μM. The results suggest that compound of **9b** exhibits a wide therapeutic safety range when it was administered to SH-SY5Y-APPsw cells. Moreover, these preliminary results could encourage further studies to explain the neuroprotective mechanisms of **9b**.

The human neuroblastoma cell line SH-SY5Y-APPsw can highly express the

APP gene after exposure by copper or other metal ions, and this model can imitate the cytotoxicity of Aβ aggregation [17]. As shown in Fig. 4b, incubation of SH-SY5Y-APPsw cells with copper caused significant toxicity, and cell viability was approximately 46% lower than that of the control group ($p < 0.005$). Compound **9b** (10 μM) treatment significantly prevented copper-induced Aβ aggregate toxicity, **9b**-treated cells displayed significantly greater viability than the cells treated only by copper ($p < 0.01$). The positive control donepezil did not prevent the cytotoxicity of Aβ aggregates induced by copper. Overall these experiments clarified the ability of compound **9b** to protect SH-SY5Y-APPsw cells from toxic Aβ species induced by copper.

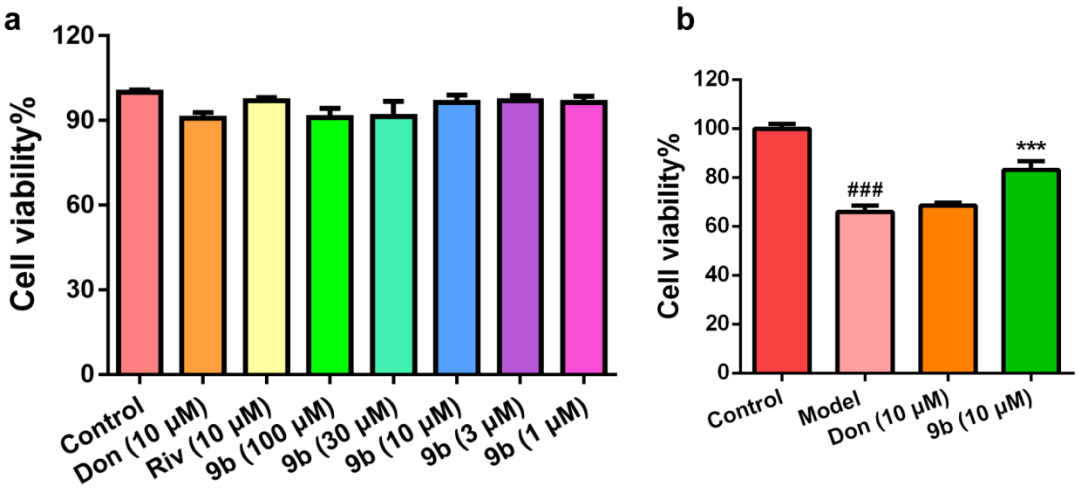

Fig. 4. MTT measurement of cell viability of compound **9b** in SH-SY5Y-APPsw cells. (**a**) Cell viability was assessed by MTT assay, SH-SY5Y-APPsw cells were treated with compound **9b** at a different concentration of 0-100 μM for 72h, the results are expressed as the percentage of viable cells. (**b**) Protective effect of compound **9b** and donepezil from copper-induced Aβ aggregation neurotoxicity. The data are shown as the mean ± SD from three different experiments, $^{###}p < 0.005$ vs. control group, $^{**}p < 0.01$ vs. the copper model group.

2.8. In vitro anti-inflammatory activity evaluation

Neuroinflammation is one of the hallmarks of AD pathogenesis. Therefore, suppression of neuroinflammatory processes may have good potential as a therapeutic

approach against AD [28-30]. Thus, compound **9b** was evaluated for its *in vitro* anti-inflammatory effects. Cell viability assay was performed to determine the cytotoxicity of **9b** on BV-2. The result indicated that **9b** (0 - 100 μM) did not show any significant effect on the proliferation of normal cultures of BV-2 in 72 h incubation time period (Fig 5a). After pretreating BV-2 cells for 1 h with **9b** and lipopolysaccharide (LPS) for 24 h, the production of interleukin-6 (IL-6) and TNF-α were determined by ELISA. As shown in Fig. 5b-c, LPS induced a significant increase in pro-inflammatory IL-6 and TNF-α ($p < 0.005$), whereas **9b** clearly suppressed the production of IL-6 and TNF-α in LPS-stimulated BV-2 microglia ($p < 0.005$). Donepezil did not display the anti-inflammatory effect.

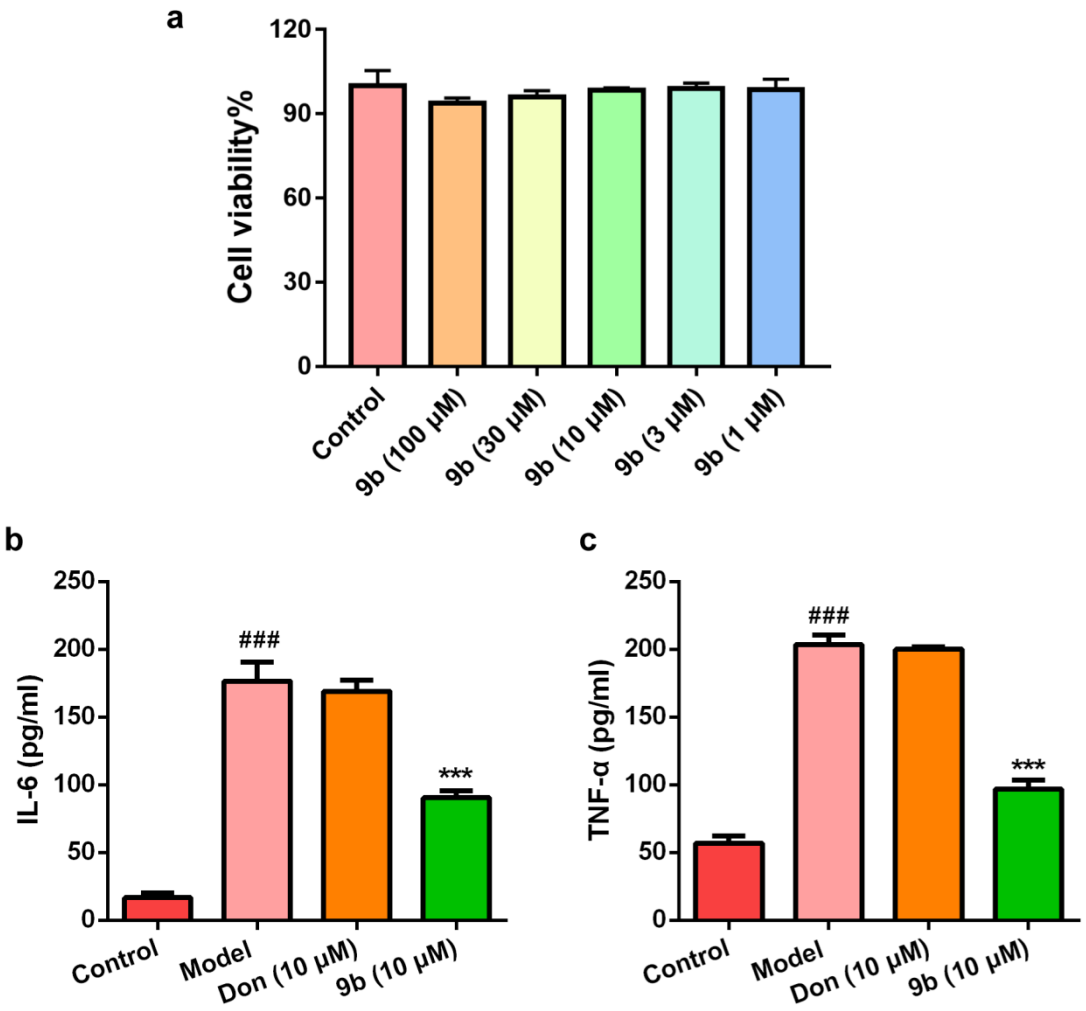

Fig. 5. Effects of **9b** on the expression of pro-inflammatory factors in LPS-stimulated BV-2 microglia. (**a**) Cell viability was assessed by MTT assay, BV-2 cells were

treated with compound **9b** at a different concentration of 1-100 μM for 72 h, the results are expressed as the percentage of viable cells. For the anti-inflammatory effects of **9b**, cells were pre-treated with **9b** at 10 μM for 1 h, and then subjected to treatment with LPS (100 ng/mL) for 24 h. The amounts of IL-6 (**b**) and TNF-α (**c**) were measured by ELISA, $^{###}$ The data are shown as the mean ± SEM from three different experiments, $p < 0.005$, vs. control group. ***$p < 0.005$, vs. model group.

*2.9. Acute toxicity of **9b***

Safety is a primary concern in the development of new drugs. The acute toxicity of compound **9b**, the most promising multifunctional anti-AD agent, was determined in ICR mice by orally administering doses of 0, 100, 200, 500, or 1000 mg/kg (n = 5 per group) [31]. After 14 days monitoring, all mice remained alive and no acute toxicity phenomena were observed, including significant abnormal behavior, altered water or food consumption, or marked body weight changes. All animals were euthanized on the 14th day and no macroscopic abnormities of the heart, liver, and kidneys were detected. These results indicate that the treated animals did not develop acute toxicity symptoms, and tolerated compound **9b** at doses up to 1000 mg/kg.

2.10. Pharmacokinetic profile and log BB value

To further understand the pharmacokinetics of **9b**, a preliminary pharmacokinetic analysis was performed in mice. Results in Table 6 display the plasma concentration of **9b** vs the time following a 30 mg/kg dose. The maximum plasma concentration (C_{max}) was 51.95 μg/L at 0.65 h (T_{max}) after of oral administration. After C_{max}, there was a slow decline and elimination beyond 48 h (Fig. 6). The approximate $T_{1/2}$ was 13.89 h. The area under curve until the last measurable concentration ($AUC_{(0-t)}$), and area under curve to infinite time ($AUC_{(0-\infty)}$) were 324.69 μg/L*h and 352.15 μg/L*h, respectively. Interestingly, the level of **9b** was 47.24 μg/L in the plasma and 762.10 μg/L in the brain after 40 min, which displayed a blood/brain partitioning (log BB) value of 1.24 ± 0.07. The log BB value indicates compound **9b** penetrated the BBB and could therefore be liable to having anti-AD effects. Overall, these *in vivo* pharmacokinetic results facilitate the evaluation of drug-like properties of **9b** as a potential AD treatment.

Table 6 Pharmacokinetic parameters of **9b**.

p.o.[a]	$T_{1/2}$(h)	T_{max} (h)	C_{max} (μg/L)	$AUC_{(0-t)}$ (μg/L*h)	$AUC_{(0-\infty)}$ (μg/L*h)
9b	13.89±2.51	0.65±0.08	51.95±12.20	324.69±31.57	352.15±32.16

p.o.[b]	plasma(μg/L)	brain(μg/L)	log BB
9b	47.24±7.80	762.10±31.56	1.24±0.07

The data are expressed as mean ± SEM.
[a] p.o., oral administration, dose is 30 mg/kg, n = 6.
[b]40 min after oral administration, dose is 30 mg/kg, n = 6.

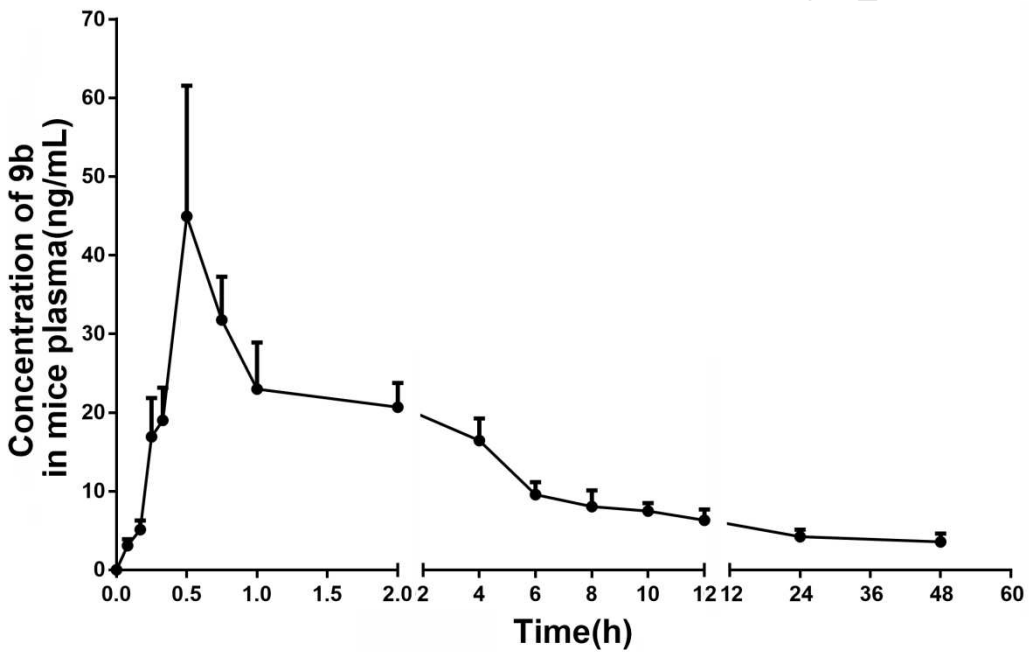

Fig. 6. Mean plasma concentration-time profiles of **9b** (30 mg/kg, p.o.) in ICR mice (n = 6). The data are expressed as mean ± SEM.

2.11. In vivo assay

Cognitive improvement is the utmost criterion for evaluating anti-AD drugs. The ability of **9b** to improve scopolamine-induced cognitive impairment in ICR mice was determined using a step-down passive avoidance test [32]. As shown in Fig. 7, in the training test there was no difference regarding the latency among the different groups. During the test stage, the latency of step-down of mice treated with scopolamine was significantly less (5 s) than that of control mice (116 s) ($p < 0.005$). Compound **9b** significantly prolonged the scopolamine-induced latency in a dose-dependent manner

(Fig. 7a). Especially, the latency of mice treated with 30 mg/kg compound **9b** was markedly greater than control mice, with latency scores of 53 seconds and 5 seconds, respectively. This indicates compound **9b** was clearly linked to improved memory in mice experiencing scopolamine-induced cognitive impairment.

Our data reveals that compound **9b**, as a multifunctional agent, might be a good potential candidate for treating AD. Our results also showed that the positive control agent donepezil demonstrated a strong therapeutic effect for scopolamine-induced mice.

The index of error time is widely used to evaluate the ability of learning and memory in animal models. Our results indicate that there was no difference regarding the error times between the different groups during the training stage. However, in the subsequent retention trial, the error times of mice treated with scopolamine alone (1 mg/kg, model group) were significantly greater than those of the vehicle-treated mice (control group) ($p < 0.01$). Compared to the model mice, the mice receiving **9b** treatment showed the less error times in a dose-dependent manner (10 mg/kg, $p < 0.05$; 30 mg/kg, $p < 0.01$; Fig 7b). These results indicate that compound **9b** might have decreased the cognitive deficit induced by scopolamine, which could be linked to an increase in brain-cholinergic activity.

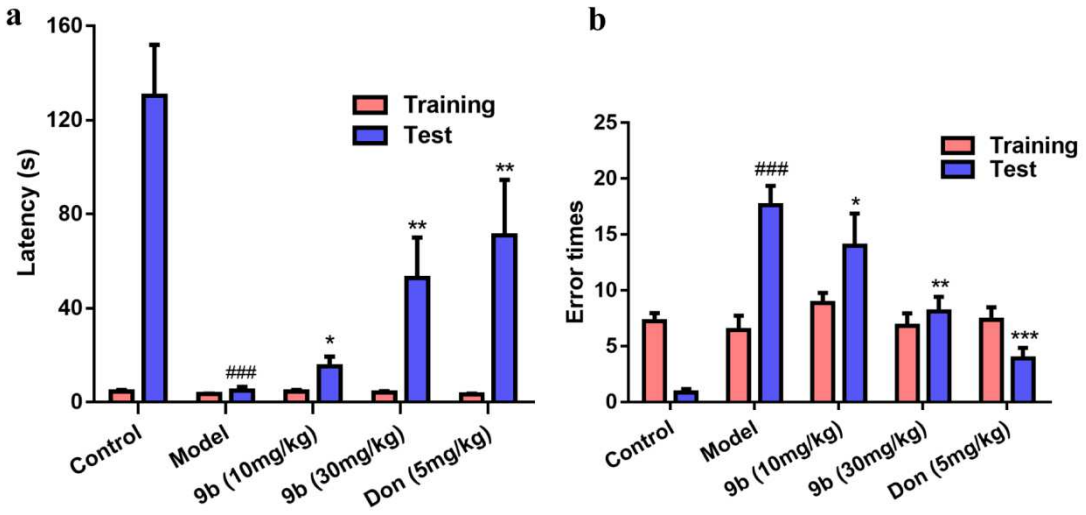

Fig. 7. Effects of compound **9b** on scopolamine-induced memory deficit by step-down passive avoidance test in mice. During the training period, no significant

differences were observed in latency and error times of mice among groups. In the test stage, the mice were pretreated with compounds **9b** (10 and 30 mg/kg, p.o.) or donepezil (5.0 mg/kg, p.o.) for 1 h, then scopolamine (3 mg/kg, i.p.) were orally given for another 30 min. Latency (**a**) and error times (**b**) were measured by step-down passive avoidance was tested. The data are shown as the mean ± SEM (n = 15). $^{###}p <$ 0.005 vs. control group. *$p < 0.05$, **$p < 0.01$ and ***$p < 0.005$ vs. the model group.

3. Conclusion

In the present work, a series of novel isoflavone analogs **2a-9c** were designed, synthesized and evaluated as multifunctional agents against AD by their targeting of H3R and AChE, and protecting neuronal cells from damage, suppressing neuroninflammatory response. The most interesting agent within our 11 compounds was **9b**, which showed an obvious multifunctional profile in blocking H3R with an IC_{50} value of 0.27 μM and significantly inhibiting activities against AChE with an IC_{50} value of 0.08 μM, but weakly inhibiting effect for BuChE (IC_{50} value of 2.89 μM). Molecular docking results provided an explanation for mix-type inhibition, as **9b** could bind simultaneously to H3R and AChE. Moreover, Compound **9b** displayed a modest antioxidant activity and obvious anti-neuroinflammatory property, exhibited a low toxicity and strong neuroprotective effects on SH-SY5Y-APPsw cells. More importantly, our *in vivo* study revealed that compound **9b** does not exhibit any acute toxicity in mice at doses up to 1000 mg/kg; also that **9b** oral treatment (10 and 30 mg/kg) significantly prevented scopolamine-induced memory deficits in mice by prolonging the latency and reducing the error times in the step-down passive avoidance test. It also possessed reasonable pharmacokinetic properties, with substantial metabolic stability ($T_{1/2}$ = 13.89 h *in vivo*) and salient log BB values (log BB = 1.24) for penetration of the CNS in mouse. Therefore, the current study suggests that compound **9b** is a reliable and promising multifunctional drug candidate for treating AD and deserves further investigation into its mechanisms of action.

4. Experimental

4.1. Chemistry

Unless otherwise indicated, all solvents and organic reagents were obtained from

commercially available sources and were used without further purification. The reaction process was monitored using ultra-performance liquid chromatography-mass spectrometry (UPLC-MS). Yields were not optimized. ^{1}H NMR spectra was recorded on a Varian Mercury-400 or 500 MHz instrument, while ^{13}C NMR was recorded on a Varian Mercury-400 or 600 MHz instrument using DMSO-d_6, $CDCl_3$, CD_3OD, or CD_3COCD_3 as a solvent and tetramethylsilane (TMS) as an internal standard (^{1}H NMR and ^{13}C NMR were recorded at different times). High-resolution mass spectra (HRMS) were recorded on an Agilent Technologies LC/MSD TOF spectrometer. Thin-layer chromatography (TLC) analysis was carried out on silica gel plates GF254 (Yantai Chemical Research Institute, China). Column chromatography was performed on silica gel (90-150 mm; Qingdao Marine Chemical Inc.).

*4.1.1. General procedure for the preparation of intermediates (**1a, 1b**)*

Formononetin (5.0 g, 18.6 mmol), finely grounded anhydrous K_2CO_3 (30 g, 217 mmol) and 1,2-dibromoethane (16.0 mL, 186 mmol) or 2,2'-dibromodiethyl ether (23.4 mL, 186 mmol) were added to 500 mL acetone. The mixture was refluxed for 10 h. The residues were then added into 100 mL water and stirred for 1 h then filtered by suction. The filter was then washed three times with 5 mL water. Finally, the solid was dried in a vacuum at 50 °C to give **1a** and **1b** without further purification.

*4.1.1.1. 7-(2-(2-Bromoethoxy)-ethoxy)-3-(4-methoxyphenyl)-4H-chromen-4-one (**1a**)*

White solid, 93% yield. mp 112.1-113.7 °C. ^{1}H NMR (400 MHz, $CDCl_3$): δ 8.21 (d, *J* = 8.8 Hz, 1H), 7.92 (s, 1H), 7.50 (d, *J* = 8.8 Hz, 2H), 7.03-6.96 (m, 3H), 6.87 (d, *J* = 2.0 Hz, 1H), 4.24 (t, *J* = 4.8 Hz, 2H), 3.95-3.89 (m, 4H), 3.84 (s, 3H), 3.51 (t, *J* = 6.0 Hz, 2H); ^{13}C NMR (100 MHz, $CDCl_3$): δ 175.9, 163.1, 159.7, 157.9, 152.2, 130.3, 128.0, 125.0, 124.3, 118.8, 114.9, 114.1, 101.1, 71.6, 69.4, 68.1, 55.5, 30.3. ESI-MS (m/z): 419.13 $[M+H]^+$.

*4.1.1.2. 7-(2-Bromoethoxy)-3-(4-methoxyphenyl)-4H-chromen-4-one (**1b**)*

White solid, 93% yield, mp 177.7-179.6 °C. Data for this compound were in

agreement with those reported in the literature [18].

*4.1.2. General procedure for the synthesis of compounds **2a-2e***

To a mixture of intermediate **1a** (1.25 g, 3.0 mmol) or **1b** (1.13 g, 3.0 mmol) and K_2CO_3 (13.8 g, 100 mmol) in 100 mL CH_3CN, the corresponding amines (6.0 mmol) and DMF (30 mL) were added, and the resulting solution was refluxed and monitored by UPLC-MS. When the reaction was finished, the reaction solution was poured into ice water and extracted with CH_2Cl_2. The combined organic layers were washed with water and dried over Na_2SO_4. After concentrated *in vacuo*, the residue was purified by column chromatography using CH_2Cl_2/MeOH (97:3) as eluents to yield the pure compounds **2a-2e** and **3**.

*4.1.2.1. 3-(4-methoxyphenyl)-7-(2-(2-(piperidin-1-yl)ethoxy)ethoxy)-4H-chromen -4-one (**2a**)*

Light yellow solid, 16％ yield. mp 138.0-139.9 °C. ^{1}H NMR (400 MHz, $CDCl_3$): δ 8.20 (d, *J* = 8.8 Hz, 1H), 7.91 (s, 1H), 7.49 (d, *J* = 8.8 Hz, 2H), 7.02-6.95 (m, 3H), 6.86 (d, *J* = 2.4 Hz, 1H), 4.22 (t, *J* = 4.8 Hz, 2H), 3.86 (t, *J* = 4.8 Hz, 2H), 3.83 (s, 3H), 3.71 (t, *J* = 6.0 Hz, 2H), 2.60 (t, *J* = 6.0 Hz, 2H), 2.45 (m, 4H), 1.62-1.56 (m, 4H), 1.45-1.39 (m, 2H) ; ^{13}C NMR (100 MHz, $CDCl_3$): δ 175.9, 163.3, 159.7, 157.9, 152.2, 130.2, 127.9, 125.0, 124.4, 118.6, 115.0, 114.1, 101.0, 69.5, 69.3, 68.2, 58.6, 55.5, 55.2, 26.0, 24.3. HRMS: $C_{25}H_{30}NO_5$ $[M+H]^+$: m/z Calcd: 424.2124; Found: 424.2124.

*4.1.2.2. 7-(2-(cyclopentylamino)ethoxy)-3-(4-methoxyphenyl)-4H-chromen-4-one (**2b**)*

Light yellow solid, 17% yield. mp 110.5-112.7 °C. ^{1}H NMR (400 MHz, CD_3OD): δ 8.23 (s, 1H), 8.13 (d, *J* = 8.8 Hz, 1H), 7.48 (d, *J* = 8.4 Hz, 2H), 7.13-7.11 (m, 2H), 6.99 (d, *J* = 8.4 Hz, 2H), 4.23 (t, *J* = 4.2 Hz, 2H), 3.83 (s, 3H), 3.20-3.13 (m, 1H), 3.04 (t, *J* = 4.2 Hz, 2H), 2.00-1.92 (m, 2H), 1.78-1.70 (m, 2H), 1.64-1.55 (m, 2H), 1.45-1.36 (m, 2H); ^{13}C NMR (100 MHz, $CDCl_3$): δ 176.0, 163.4, 159.7, 158.0, 152.2, 130.3, 127.9, 125.0, 124.4, 118.6, 114.9, 114.1, 100.8, 68.6, 59.9, 55.5, 47.4, 33.4, 24.2. HRMS: $C_{23}H_{26}NO_4$ [M+H]+: m/z Calcd: 380.1862; Found: 380.1861.

*4.1.2.3. 2-(2-((3-(4-methoxyphenyl)-4-oxo-4H-chromen-7-yl)oxy)ethyl)isoindoline-1, 3-dione (**2c**)*

White solid, 82% yield. mp 170.8-172.5 °C. ^{1}H NMR (400 MHz, DMSO-d_6): δ 8.40 (s, 1H), 7.99 (d, *J* = 8.8 Hz, 1H), 7.90-7.83 (m, 4H), 7.51 (d, *J* = 8.8 Hz, 2H), 7.17 (d, *J* = 2.4 Hz, 1H), 7.02-6.98 (m, 3H), 4.39 (t, *J* = 5.6 Hz, 2H), 4.02 (t, *J* = 5.6 Hz, 2H), 3.78 (s, 3H) ; ^{13}C NMR (100 MHz, DMSO-d_6): δ 174.6, 167.7, 162.3, 159.0, 157.3, 153.5, 134.5, 131.5, 130.1, 127.0, 124.0, 123.4, 123.2, 117.8, 115.1, 113.6, 101.2, 65.5, 55.1, 36.7. HRMS: $C_{26}H_{20}NO_6$ [M+H]+: m/z Calcd: 442.1291; Found: 442.1282.

*4.1.2.4. 7-(2-(cyclohexylamino)ethoxy)-3-(4-methoxyphenyl)-4H-chromen-4-one (**2d**)*

Light yellow solid, 74% yield. mp 119.2-121.7 °C. ^{1}H NMR (400 MHz, $CDCl_3$): δ 8.20 (d, *J* = 8.8 Hz, 1H), 7.91 (s, 1H), 7.50 (d, *J* = 8.4 Hz, 2H), 7.01-6.96 (m, 3H), 6.85 (d, *J* = 2.4 Hz, 1H), 4.17 (t, *J* = 4.2 Hz, 2H), 3.84 (s, 3H), 3.09 (t, *J* = 4.2 Hz, 2H), 2.55-2.48 (m, 1H), 1.95-1.92 (m, 2H), 1.79-1.75 (m, 2H), 1.66-1.63 (m, 2H), 1.34-1.07 (m, 4H); ^{13}C NMR (100 MHz, $CDCl_3$): δ 176.0, 163.4, 159.7, 158.0, 152.2, 130.3, 127.9, 125.1, 124.4, 118.7, 114.9, 114.1, 100.9, 68.8, 56.9, 55.5, 45.7, 33.8, 26.3, 25.2. HRMS: $C_{24}H_{28}NO_4$ $[M+H]^+$: m/z Calcd: 394.2018; Found: 394.2012.

*4.1.2.5. Tert-butyl (2-((3-(4-methoxyphenyl)-4-oxo-4H-chromen-7-yl)oxy)ethyl) carbamate (**2e**)*

White solid, 96% yield. mp 98.6-101.9 °C. ^{1}H NMR (400 MHz, CD_3COCD_3): δ 8.23 (s, 1H), 8.11 (d, *J* = 8.0 Hz, 1H), 7.57 (d, *J* =7.6 Hz, 2H), 7.08 (d, *J* = 7.6 Hz, 2H), 6.99 (d, J = 8.0 Hz, 2H), 4.24 (t, J = 5.6 Hz, 2H), 3.84 (s, 3H), 3.56-3.52 (m, 2H), 1.42 (s, 9H); ^{13}C NMR (100 MHz, CD_3COCD_3): δ 175.6, 164.2, 160.5, 158.7, 156.8, 153.6, 131.0, 128.1, 125.4, 125.1, 119.2, 115.7, 114.4, 101.7, 79.0, 68.5, 55.6, 40.5, 28.6. HRMS: $C_{23}H_{26}NO_6$ $[M+H]^+$: m/z Calcd: 412.1760; Found: 412.1747.

*4.1.3. 7-(2-aminoethoxy)-3-(4-methoxyphenyl)-4H-chromen-4-one hydrochloride (**3**)*

Compound **2e** (0.41 g, 1.00 mmol) was stirred in hydrochloride ethanol solution (30ml, 30-40%) at room temperature for 20 min. The mixture was evaporated to dryness under reduced pressure. The residue was washed with acetone twice to give the title compound as a white solid, 82% yield. mp>250 °C. ^{1}H NMR (400 MHz, CD_3OD): δ 8.24 (s, 1H), 8.17 (d, *J* = 9.2 Hz, 1H), 7.49 (d, *J* = 8.8 Hz, 2H), 7.19-7.16 (m, 2H), 7.00 (d, *J* = 9.2 Hz, 2H), 4.39 (t, *J* = 5.2 Hz, 2H), 3.83 (s, 3H), 3.44 (t, *J* = 5.2 Hz, 2H); ^{13}C NMR (100 MHz, CD_3OD): δ 177.9, 164.1, 161.3, 159.5, 155.1, 131.4, 128.6, 126.1, 125.2, 119.8, 116.2, 114.9, 102.5, 66.1, 55.8, 40.1. HRMS: $C_{18}H_{18}NO_4$ $[M+H]^+$: m/z Calcd: 312.1236; Found: 312.1235.

*4.1.4. 2-aminobenzoic acid (**4**)*

A solution of 2-nitrobenzoic acid (8.00 g, 47.9 mmol) in methanol (120 mL) was added to Pd/C, and the resulting mixture was stirred under hydrogen atmosphere at room temperature for 8 h. The resulting mixture was filtered and the filtrate was concentrated *in vacuo* to give the desired product **4** as a light yellow solid in yield of 43%. mp 140.8-142.8 °C. ^{1}H NMR (400 MHz, CD_3OD): δ 7.80 (dd, *J* = 6.4, 1.2 Hz, 1H), 7.24-7.20 (m, 1H), 6.72 (d, *J* = 6.4 Hz, 1H), 6.58-6.55 (m, 1H); ^{13}C NMR (100 MHz, CD_3OD): δ171.7, 152.8, 134.9, 132.7, 117.7, 116.6, 111.9. ESI-MS (m/z): 138.04 $[M+H]^+$.

*4.1.5. 9-chloro-1,2,3,4-tetrahydroacridine (**5**)*

A mixture of **4** (2.06 g, 15 mmol) and cyclohexanone (1.55 mL, 15 mmol) was added to phosphorus oxychloride (15 mL, 164 mmol) in an ice bath for 2 min, then the mixture was refluxed for 1 h. After evaporation of the solvent, the residue was dissolved in dichloromethane (10 mL). The combined organic phases were washed with potassium carbonate solution and saturated aqueous sodium chloride, dried over sodium sulfate, and filtered. The filtrate was evaporated to dryness under reduced pressure. The residue was recrystallized from acetone to give the **5** as a yellow solid in yield of 57%. mp 67.0-68.0 °C. ^{1}H NMR (400 MHz, $CDCl_3$): δ 8.16 (d, *J* = 8.4 Hz, 1H), 7.98 (d, *J* = 8.8 Hz, 1H), 7.68-7.64 (m, 1H), 7.55-7.51 (m, 1H), 3.14-3.11 (m,

2H), 3.04-3.01 (m, 2H), 1.98-1.92 (m, 4H); ^{13}C NMR (100 MHz, $CDCl_3$): δ 159.6, 146.8, 141.6, 129.4, 129.0, 128.7, 126.6, 125.5, 123.8, 34.3, 27.6, 22.8, 22.8. ESI-MS (m/z): 218.16 $[M+H]^+$.

*4.1.6. 3-(4-methoxyphenyl)-7-(2-((1,2,3,4-tetrahydroacridin-9-yl)amino)ethoxy)-4H-chromen-4-one (**6**)*

The compound **3** (1.40 g,4.04 mmol) was dissolved in water and an aqueous solution of sodium hydroxide (10%) was added dropwise to the mixture until the aqueous solution became basic. The mixture was extracted with dichloromethane (20 mL). The combined organic phases were washed with saturated aqueous sodium chloride (30 mL), dried over sodium sulfate, and filtered. The solvent was evaporated to dryness under reduced pressure. The residue was added to compound **5** (0.88 mg, 4.04 mmol), phenol (2.30 g, 24.4 mmol) and NaI (0.10 mg, 0.67 mmol). The reaction mixture was warmed to 180-185 °C and stirred for 2 h under an argon atmosphere. When the reaction was over (TLC analysis), ethyl acetate was added and the organic layer was washed with aqueous sodium hydroxide,water, then saturated aqueous sodium chloride, then dried over sodium sulfate and filtered. The solvent was evaporated to dryness under reduced pressure. The residue was purified on a silica gel chromatography using dichloromethane/ethyl acetate (20:1) as eluent to produce the light yellow solid in the yield of 52%. mp 149.7-152.3 °C. ^{1}H NMR (400 MHz, CD_3OD): δ 8.18-8.15 (m, 2H), 8.06 (d, *J* = 8.8 Hz, 1H), 7.79 (d, *J* = 8.4 Hz, 1H), 7.58 (t, *J* = 7.6 Hz, 1H), 7.47 (d, *J* = 8.4 Hz, 2H), 7.40 (t, *J* = 7.6 Hz, 1H), 6.99 (d, *J* = 8.4 Hz, 2H), 6.93-6.93 (m, 2H), 4.25 (t, *J* = 4.8 Hz, 2H), 3.98 (t, *J* = 4.8 Hz, 2H), 3.83 (s, 3H), 2.99 (t, *J* = 6.0 Hz, 2H), 2.81 (t, *J* = 6.0 Hz, 2H), 1.90-1.85 (m, 4H); ^{13}C NMR (100 MHz, CD_3OD): δ 175.9, 162.7, 159.8, 159.0, 157.9, 152.2, 149.7, 147.5, 130.2 (2C), 129.1, 128.6, 128.2, 125.1, 124.5, 124.2, 122.5, 121.1, 119.0, 118.6, 114.7, 114.1 (2C), 101.0, 68.2, 55.5, 48.1, 34.2, 24.8, 23.1, 22.9. HRMS: $C_{31}H_{29}N_2O_4$ $[M+H]^+$: m/z Calcd: 493.2127; Found: 493.2115.

*4.1.7. General procedure for the synthesis of **A–E***

Compounds **A–E** were synthesized according to our previously reported method and the spectral data were matched with our previous publication [18].

*4.1.8. General procedure for the synthesis of **7a–7c***

Compound **A** (4.08 g, 10 mmol), **B** (3.81 g, 10 mmol) or **E** (3.79 g, 10 mmol) was added into 60 mL 40% hydrobromic acid. After stirring at 120 °C for 3 h, the reaction mixture was cooled to 0 °C and filtered. The filtered residue was purified by recrystallization with methanol to give pure intermediate **7a**–**7c**.

*4.1.8.1. 3-(4-hydroxyphenyl)-7-(4-(piperidin-1-yl)butoxy)-4H-chromen-4-one hydrobromide (**7a**)*

Off-white solid, 81% yield. mp 225.3-228.5 °C. ^{1}H NMR (400 MHz, D_2O/CD_3OD): δ 8.15 (s, 1H), 8.02 (d, *J* = 8.8 Hz, 1H), 7.38 (d, *J* = 8.0 Hz, 2H), 7.06-6.94 (m, 4H), 4.10 (t, *J* = 4.8 Hz, 2H), 3.54 (m, 2H), 3.16 (m, 2H), 2.94 (t, *J* =10.8 Hz, 2H), 2.00-1.72 (m, 10H); ^{13}C NMR (100 MHz, D_2O/CD_3OD): δ 178.6, 164.7, 159.3, 157.4, 155.3, 131.4, 127.9, 125.4, 124.3, 118.4, 116.6, 116.3, 101.9, 69.0, 57.6, 54.2, 26.7, 23.9, 22.3, 21.6. HRMS: $C_{24}H_{28}NO_4$ $[M+H]^+$: m/z Calcd: 394.2018; Found: 394.2019.

*4.1.8.2. 7-(4-(ethyl(methyl)amino)butoxy)-3-(4-hydroxyphenyl)-4H-chromen-4-one hydrobromide (**7b**)*

White solid, 76% yield. mp 234.4-236.8 °C. ^{1}H NMR (500 MHz, DMSO-d_6): δ 8.38 (s, 1H), 8.02 (d, *J* = 9.0 Hz, 1H), 7.39 (d, *J* = 8.5 Hz, 2H), 7.14 (d, *J* = 2.0 Hz, 1H), 7.10 (dd, *J* = 9.0 Hz, *J* =2.0 Hz, 1H), 6.84 (d, *J* = 8.5 Hz, 2H), 4.14 (t, *J* = 6.5 Hz, 2H), 2.31 (m, 4H), 2.12 (s, 1H), 1.79-1.73 (m, 2H), 1.59-1.53, 0.97 (t, *J* = 7.5 Hz, 3H) ; ^{13}C NMR (125 MHz, DMSO-d_6): δ 175.4, 163.7, 158.1(2C), 153.8, 130.7 (2C), 130.3, 127.6, 124.3, 122.8, 118.1, 115.7 (2C), 114.0, 101.6, 69.1, 56.8, 51.5, 41.8, 27.0, 23.8, 12.8. HRMS: $C_{22}H_{26}NO_4$ $[M+H]^+$: m/z Calcd: 368.4530; Found: 368.4525.

4.1.8.3. 3-(4-hydroxyphenyl)-7-(2-(piperidin-1-yl)ethoxy)-4H-chromen-4-one

*hydrobromide (**7c**)*

White solid, 60 mg, 21% yield. mp 241.2-246.5°C. ^{1}H NMR (400 MHz, DMSO-d_6):δ 8.39 (s, 1H), 8.04 (d, *J* = 8.8Hz, 1H), 7.40 (d, *J* = 8.0Hz, 2H), 7.21 (s, 1H), 7.10 (d, *J* = 8.8Hz, 1H), 6.82 (d, *J* = 8.0Hz, 2H), 4.34 (t, *J* = 4.2Hz, 2H), 3.03 (t, *J* = 4.2Hz, 2H), 2.77 (m, 4H), 1.64-1.58 (m, 4H) , 1.44 (m, 2H) ; ^{13}C NMR (100 MHz, DMSO-d_6): δ 178.7, 163.4, 159.2, 157.4, 155.5, 131.5, 128.2, 125.6, 124.2, 119.1, 116.4, 116.4, 102.4, 63.3, 56.4, 54.7, 23.7, 22.1. HRMS: $C_{22}H_{24}NO_4$ $[M+H]^+$: m/z Calcd: 366.1705; Found: 366.1694.

*4.1.9. General procedure for the synthesis of intermediates **8a–8c***

The suspension of intermediate **7a** (2.37 g, 5.0 mmol) or **7b** (2.24 g, 5.0 mmol) or **7c** (2.23 g, 5.0 mmol) was stirred at 70 °C for 2 d in potassium carbonate (4.15 g, 30 mmol) and 1,2-dibromoethane (2.16 mL, 25 mmol). Then the solvent was evaporated under vacuum. Water (50 mL) was added to the residue. The precipitate was filtered and washed twice with water. The crude product was dried in an oven and used in the next step without further purification.

*4.1.10. General procedure for the synthesis of target compounds **9a-9c***

The suspension of compound **8a** (1.00 g, 2.0 mmol) or **8b** (0.95 g, 2.0 mmol) or **8c** (0.94 g, 2.0 mmol) was stirred at 100 °C for 2h with potassium carbonate (2.76 g, 20 mmol) and piperidine (1.82 mL, 20 mmol) in acetonitrile (50 mL). Then the reaction mixture was poured into ice water and then filtered. The filtered residues were dried in an oven and purified by column chromatography using DCM/MeOH (20:3) as eluent to yield target compounds **9a-9c**.

*4.1.10.1 7-(4-(piperidin-1-yl)butoxy)-3-(4-(2-(piperidin-1-yl)ethoxy)phenyl)-4H-chromen-4-one (**9a**)*

Light yellow solid, 75% yield. mp 127.6-130.6 °C. ^{1}H NMR (400MHz, $CDCl_3$): δ 8.19 (d, *J* = 8.4 Hz, 1H), 7.91 (s, 1H), 7.48 (d, *J* = 8.4 Hz, 2H), 6.97 (m, 3H), 6.83 (d, *J* = 2.0 Hz, 1H), 4.14 (t, *J* = 8.4 Hz, 2H), 4.08 (t, *J* = 8.4 Hz, 2H), 2.79 (t, *J* = 8.4 Hz,

2H), 2.52 (m, 4H), 2.39-2.35 (m, 6H), 1.89-1.82 (m, 2H), 1.73-1.66 (m, 2H), 1.64-1.56 (m, 8H),1.48-1.41 (m, 4H) ; ^{13}C NMR (100 MHz, $CDCl_3$): δ 176..0, 163.6, 159.0, 158.1, 152.1, 130.2 (2C), 127.8, 125.0, 124.5, 118.4, 115.0, 114.8 (2C), 100.7, 68.7, 66.2, 58.1, 58.1, 55.2 (2C), 54.8 (2C), 27.3, 26.2, 26.1, 24.7, 24.3, 23.6. HRMS: $C_{31}H_{41}N_2O_4$ $[M+H]^+$: m/z Calcd: 505.3066; Found: 505.3065.

*4.1.10.2. 7-(4-(ethyl(methyl)amino)butoxy)-3-(4-(2-(piperidin-1-yl)ethoxy)phenyl)-4H-chromen-4-one (**9b**)*

White solid, 71% yield. mp 127.6-130.6 °C. ^{1}H NMR (500 MHz, $CDCl_3$): δ 8.19 (d, *J* = 9.0Hz, 1H), 7.91 (s, 1H), 7.48 (dd, *J* = 7.0 Hz, *J* = 2.0 Hz 2H), 6.98-6.96 (m, 3H), 6.83 (d, *J* = 2.5 Hz, 1H), 4.15 (t, *J* = 6.0 Hz, 2H), 4.08 (t, *J* = 6.5 Hz, 2H), 2.80 (t, *J* = 6.0Hz, 2H), 2.52 (m, 4H), 2.42-2.49 (m, 4H), 2.26 (s, 1H), 1.84-1.88 (m, 2H), 1.73-1.67 (m, 2H), 1.64-1.60 (m, 2H), 1.47-1.42 (m, 2H), 1.09 (t, *J* = 7.0 Hz, 3H); ^{13}C NMR (125 MHz, DMSO-d_6): δ 175.8, 163.4, 158.8, 157.9.1, 152.1, 130.1 (2C), 127.7, 124.8, 124.3, 118.3, 114.8, 114.6 (2C), 100.6, 68.4, 66.0, 57.9, 56.8, 55.1 (2C), 51.4, 41.5, 27.0, 26.0 (2C), 24.1, 23.8, 12.22. HRMS: $C_{29}H_{39}N_2O_4$ $[M+H]^+$: m/z Calcd: 479.2910; Found: 479.2902.

*4.1.10.3. 7-(2-(piperidin-1-yl)ethoxy)-3-(4-(2-(piperidin-1-yl)ethoxy)phenyl)-4H-chromen- 4-one (**9c**)*

White solid, 54% yield. mp 148.7-152.2 °C. ^{1}H NMR (400 MHz, $CDCl_3$): δ 8.19 (d, *J* = 9.2 Hz, 1H), 7.91 (s, 1H), 7.48 (d, *J* = 8.8 Hz, 2H), 7.00-6.96 (m, 3H), 6.86 (d, *J* = 2.4 Hz, 1H), 4.20 (t, *J* = 6.0 Hz, 2H), 4.15 (t, *J* = 6.0 Hz, 2H), 2.84-2.79 (m, 4H), 2.53 (m, 8H), 1.65-1.59 (m, 8H), 1.46 (m, 4H); ^{13}C NMR (100 MHz, $CDCl_3$): δ 176.0, 163.3, 158.9, 158.0, 152.2, 130.2, 127.9, 125.0, 124.4, 118.6, 115.1, 114.8, 100.9, 66.9, 66.1, 58.0, 57.8, 55.3, 55.2, 26.1, 26.0, 24.3, 24.3. HRMS: $C_{29}H_{37}N_2O_4$ $[M+H]^+$: m/z Calcd: 477.2753; Found: 477.2743.

4.2. Molecular modeling

The X-ray structures of AChE (PDB: 1EVE) was downloaded from the PDB.

Firstly, all the water molecules and irrelevant ligands were removed from the crystal structures. Then the structures were prepared with the "Clean Protein" module of Discovery Studio 2016. As a result, hydrogen atoms were added, chain termini were modified, incomplete residues were repaired and the whole protein structure was protonated at the pH of 7.0. All the water molecules were removed from the crystal structures. The previously built homology model of H3R [19] was directly used for molecular docking. GOLD (version 3.0.1, Cambridge Crystallographic Data Center, Cambridge, UK) was the program for molecular docking in this study. The settings for all the three docking simulations were the same. The binding site was defined as a sphere centered on the cognate ligand with a radius of 10Å. The times for molecular docking were set to 20. The scoring function to predict protein-ligand affinity was GoldScore. The binding poses generated by GOLD were visually inspected and the plausible binding pose was retained.

4.3. Biology

4.3.1. In vitro assay on histamine 3 receptor (H3R)

The cell-based histamine 3 receptor (H3R) assay was performed based on β-lactamase complementation technology according to the kit protocol. H3-bla U2OS cells (Invitrogen, USA) stably express two fusion proteins as well as a β-lactamase (bla) reporter gene under the control of an upstream activation sequence (UAS) response element. The first fusion protein is human H3R linked to a Gal4-VP16 transcription factor via the TEV protease site, and the other is the β-arrestin/TEV protease fusion protein. U2OS cells were seeded in a 384-well format plate (10000 cells/well) to culture with FreeStyle Expression Medium (Invitrogen, USA) for 18 h. Cells were exposed to 4 μL of tested compounds and the control compound of thioperamide (Sigma-Aldrich, USA) for 30 min, then 4 μL of 400 nM methylhistamine (Sigma-Aldrich, USA) was added to stimulate the cells. After 5 h, 8 μL of LiveBLAzer-FRET B/G Substrate (Invitrogen, USA) was added to cells for another 2 h before fluorescence detection. Fluorescence values were measured at 460 nm excitation with 530 nm emission using a BioTek Synergy H1 microplate reader,

and the inhibition percentage was plotted against the indicated concentrations of compounds. Each concentration was analyzed in triplicate, and IC_{50} values were graphically determined from log concentration−inhibition curves.

4.3.2. In vitro inhibition of AChE and BuChE

AChE and BuChE were obtained from the mouse brain and plasma, respectively. Cholinesterase inhibitory activity was measured according to Ellman's method with slight modifications [23]. The compounds were dissolved in DSMO (final reactive concentration of DMSO less than 0.1%) and diluted in 5 serial concentrations in 0.05 M phosphate buffer (PBS, pH 8.0). The reaction was performed in 96-well plates, and in each well of the plate, 80 μL of DTNB (Sigma-Aldrich, USA), 20 μL of 0.05 M PBS (pH 8.0) and20 μL of AChE or 20 μL of BuChE were incubated with 20 μL of tested compounds at their diluted concentrations at 37 °C for 30 min. After incubation, 60 μL of 3.75 mM acetylthiocholine iodide (Sigma-Aldrich, USA) or S-butyrylthiocholine iodide (Sigma-Aldrich, USA) was added as the substrate to initiate reactions, and the absorbance intensity was monitored at 412 nm using a microplate reader (Synergy H1, BioTek, USA). Donepezil and rivastigmine were used as reference compounds for AChE and BuChE, respectively. IC_{50} values were graphically determined from log concentration−inhibition curves.

4.3.3. ORAC-FL assay

The antioxidant capacity was performed using an oxygen radical absorbance capacity-fluorescein (ORAC-FL) assay according to a previously described method [25, 26] with the following modifications. Briefly, PBS (75 mM, pH 7.4) was used as reaction buffer and diluent in the experiment. The tested compounds (20 μL) and fluorescein (FL, 20 μL, 20 nM, final concentration) were mixed and preincubated for 15 min at 37 °C. Then, 140 μL of 2,2'-azobis(2-methylpropionamidine) dihydrochloride (AAPH) solution (18 mM, final concentration) was rapidly added and the fluorescence was recorded every two minutes for 160 min (460 nm excitation, 520 nm emission) by a microplate reader (Synergy H1, BioTek, USA). All the reaction

mixtures were prepared in duplicate, and at least three independent assays were performed for each sample. Antioxidant curves (fluorescence versus time) were normalized to the curve of the blank. The area under the fluorescence decay curve (AUC) was calculated as the reference described.

4.3.4. Cytotoxicity evaluation and Cell viability assay

Human neuroblastoma cells (SH-SY5Y) and SH-SY5Y-APPsw (overexpressing the Swedish mutant form human APP) were selected to determine the cytotoxicity and cell viability of the compounds by 3-(4,5-dimethylthiazol-2-yl)-2,5-diphenyltetrazolium bromide (MTT) assay, respectively. As previously described [17], cells (SH-SY5Y or SH-SY5Y-APPsw, 1×10^5/mL/100 μL/well) were incubated with test compounds (0 - 100 μM) at 37 °C in a CO_2 incubator. After 72 h of incubation, 10 μL of MTT reagent (5 mg/mL) in PBS medium was added to each well and incubated for another 4 h. Then, the medium was discarded and replaced with 150 μL DMSO to solubilize the formazan crystal. The absorbance at 490 nm was measured using a microplate reader (Synergy H1, BioTek, USA). The selectivity index (SI) for each compound was calculated as the ratio between cytotoxicity (CC_{50}, 50% cytotoxic concentration) in SH-SY5Y and inhibitory activity (IC_{50}) against H3R, AChE or BuChE.

4.3.5 Neuroprotective assay

SH-SY5Y-APPsw cells, as an AD cell model by using copper trigger the neurotoxicity of Aβ, were cultured to determine the neuroprotection of compound **9b.** Cells were treated with **9b** (10 μM) and donepezil (10 μM, positive agent) for 2 h, then the $CuSO_4$ solution (250 μM, final concentration) was added to culture for another 24 h. The cell viability was measured by MTT as above described [17].

4.3.6. LPS-induced inflammation

The immortalized mouse BV-2 microglial cell lines were used to investigate the anti-inflammatory effect of **9b** as previously described [33]. The BV-2 cells (1×10^5

cells per well in a 48-well plate) were pretreated with **9b** (10 μM) and donepezil (10 μM, positive agent) for 1 h, and then LPS (100 ng/mL) was added to stimulate for another 24 h. The cultured supernatants were collected to determine the contents of IL-6 or TNF-α by enzyme-linked immunosorbent assay (ELISA), according to the procedure recommended by the supplier (BD Biosciences, USA).

4.3.7. Pharmacokinetic analysis and log BB value studies

Preliminary pharmacokinetic properties of **9b** were studied in ICR mice, which were purchased from the laboratory animal center of Beijing Huafukang Biological Technology Co., Ltd. With a body weight of 20-22g. Male mice (n = 6) were fasted overnight and received a single dose (30 mg/kg) of **9b** (dissolved in 5% DMSO and 95% sodium carboxyl methyl cellulose) by oral gavage. Blood samples (50 μL) were obtained from orbital venous sinus at 0 min, 5 min, 10 min, 20 min, 30 min, 45 min, 1 h, 2 h, 4 h, 6 h, 8 h, 10 h, 12 h, 24 h and 48 h after the compound administration. The concentration of the corresponding compound in blood was analyzed by LC‒MS/MS (8050, Shimadzu, Japan), and pharmacokinetic parameters were processed by the software DAS 3.0 through inputting each time point and its corresponding compound's concentration. For the log BB value studies, ICR mice (n = 5) were administrated orally with a single dosage of **9b** (30 mg/kg). 40 min after the oral administration of compound **9b**, the mouse was sacrificed, the plasma and brains were collected, and the concentration of the corresponding compound in blood and brain was analyzed by LC-MS/MS. Log BB value was calculated by log the ratio of concentration in the brain to concentration in the blood.

*4.3.8. Acute toxicity of compound **9b***

A total of twenty-five ICR mice (male, 22 days, 20−22 g), purchased from the laboratory animal center of Beijing Huafukang Biological Technology Co., Ltd., were used to evaluate the acute toxicity of compound **9b**. Mice were fed standard laboratory chow and water *ad libitum*, and were kept under a 12 h dark/light cycle. The experimental procedures were approved by the Experimental Animal Care and

Use Committee of the Institute of Materia Medica, Chinese Academy of Medical Sciences & Peking Union Medical College. Different concentrations of compound **9b** were dissolved in a 0.5% carboxymethyl cellulose sodium (CMC-Na) salt solution and orally administered to different experimental groups (n = 5). After administration of the compound, the mice were continuously observed for the first 4 h for any abnormal behavior and mortality changes, intermittently for the next 24 h, and occasionally thereafter for 14 days for the onset of any delayed effects. All animals were euthanized on the 14th day after drug administration.

4.3.9. Step-down passive avoidance test

The step-down passive avoidance test was used to evaluate the cognitive ability of tested compounds on scopolamine (Sigma, USA) induced animal memory dysfunction [32]. A total of 75 ICR mice (six weeks old, 18-22 g, either gender, n = 15) were used to perform the assay and fed as described in 4.2.8. section. The apparatus consisted of a box with electric grid and a centrally located wooden platform as shock free zone. An appropriate voltage, current and time (20 V, 0.5 mA, 2 s) for foot shock was selected, the mouse was put on the electric grid and the experiment was started. The mice underwent two separate trials including a training trial and a test trial 24 h later. For the training trial, each mouse was allowed to get familiar with the chamber for 5 min. The power was then switched on and the mouse was placed on the platform. Once the mouse stepped down, it would receive an electric shock, which caused it to return to the platform. Compounds **9b** (10 and 30 mg/kg, p.o.) or donepezil (5.0 mg/kg, p.o., positive control drug) were orally administrated 2 h before each training trial. 30 min before the trial, scopolamine (1 mg/kg, i.p.) was administered to induce memory impairment. The latency to step down to the grid for the first time and the error times that number of shocks received within 5 min were measured to evaluate the cognitive ability. All data are expressed as the mean ± SEM. Differences between groups were examined for statistical significance using one-way ANOVA with Student's *t*-test. A P-value less than 0.05 denoted the presence of a statistically significant difference.

Conflicts of interest

The authors declared that they have no conflicts of interest.

Acknowledgments

This work was supported by the Beijing Municipal Natural Science Foundation (No. 7172141, 7182115), the National Natural Science Foundation of China (81573445, 81503339), The Drug Innovation Major Project of China (No. 2018ZX09711001-003-001), Beijing Key Laboratory of New Drug Mechanisms and Pharmacological Evaluation Study (BZ0150), CAMS Innovation Fund for Medical Science (2017-I2M-3-011).

References

[1] 2016 Alzheimer's disease facts and figures, Alzheimers Dement. 12 (2016) 459-509.

[2] C. Reitz, C. Brayne, R. Mayeux, Epidemiology of Alzheimer disease, Nat. Rev. Neurol. 7 (2011) 137.

[3] K. Chiang, E.H. Koo, Emerging therapeutics for Alzheimer's disease, Annu. Rev. Pharmacol Toxicol. 54 (2014) 381-405.

[4] T.E. Golde, S.T. DeKosky, D. Galasko, Alzheimer's disease: The right drug, the right time, Science 362 (2018) 1250-1251.

[5] D. Knez, N. Coquelle, A. Pislar, S. Zakelj, M. Jukic, M. Sova, J. Mravljak, F. Nachon, X. Brazzolotto, J. Kos, J.P. Colletier, S. Gobec, Multi-target-directed ligands for treating Alzheimer's disease: Butyrylcholinesterase inhibitors displaying antioxidant and neuroprotective activities, Eur. J. Med. Chem. 156 (2018) 598-617.

[6] Z. Wang, J. Hu, X. Yang, X. Feng, X. Li, L. Huang, A.S.C. Chan, Design, Synthesis, and Evaluation of Orally Bioavailable Quinoline-Indole Derivatives as Innovative Multitarget-Directed Ligands: Promotion of Cell Proliferation in the Adult

Murine Hippocampus for the Treatment of Alzheimer's Disease, J. Med. Chem. 61 (2018) 1871-1894.

[7] M. Chioua, E. Buzzi, I. Moraleda, I. Iriepa, M. Maj, A. Wnorowski, C. Giovannini, A. Tramarin, F. Portali, L. Ismaili, P. Lopez-Alvarado, M.L. Bolognesi, K. Jozwiak, J.C. Menendez, J. Marco-Contelles, M. Bartolini, Tacripyrimidines, the first tacrine-dihydropyrimidine hybrids, as multi-target-directed ligands for Alzheimer's disease, Eur. J. Med. Chem. 155 (2018) 839-846.

[8] Y.X. Xu, H. Wang, X.K. Li, S.N. Dong, W.W. Liu, Q. Gong, T.D. Wang, Y. Tang, J. Zhu, J. Li, H.Y. Zhang, F. Mao, Discovery of novel propargylamine-modified 4-aminoalkyl imidazole substituted pyrimidinylthiourea derivatives as multifunctional agents for the treatment of Alzheimer's disease, Eur. J. Med. Chem. 143 (2018) 33-47.

[9] X. Zha, D. Lamba, L. Zhang, Y. Lou, C. Xu, D. Kang, L. Chen, Y. Xu, L. Zhang, A. De Simone, S. Samez, A. Pesaresi, J. Stojan, M.G. Lopez, J. Egea, V. Andrisano, M. Bartolini, Novel Tacrine-Benzofuran Hybrids as Potent Multitarget-Directed Ligands for the Treatment of Alzheimer's Disease: Design, Synthesis, Biological Evaluation, and X-ray Crystallography, J. Med. Chem. 59 (2016) 114-131.

[10] M. Eghtedari, Y. Sarrafi, H. Nadri, M. Mahdavi, A. Moradi, F. Homayouni Moghadam, S. Emami, L. Firoozpour, A. Asadipour, O. Sabzevari, A. Foroumadi, New tacrine-derived AChE/BuChE inhibitors: Synthesis and biological evaluation of 5-amino-2-phenyl-4H-pyrano[2,3-b]quinoline-3-carboxylates, Eur. J. Med. Chem. 128 (2017) 237-246.

[11] C. Qi, Y. Qiao, W. Gao, M. Liu, Q. Zhou, C. Chen, Y. Lai, Y. Xue, J. Zhang, D. Li, J. Wang, H. Zhu, Z. Hu, Y. Zhou, Y. Zhang, New 3,5-dimethylorsellinic acid-based meroterpenoids with BACE1 and AchE inhibitory activities from Aspergillus terreus, Org. Biomol. Chem. 16 (2018) 9046-9052.

[12] A. Contestabile, The history of the cholinergic hypothesis, Behav. Brain Res. 221 (2011) 334-340.

[13] B. Sadek, A. Saad, A. Sadeq, F. Jalal, H. Stark, Histamine H3 receptor as a potential target for cognitive symptoms in neuropsychiatric diseases, Behav. Brain Res. 312 (2016) 415-430.

[14] M.I. Martinez-Mir, H. Pollard, J. Moreau, J.M. Arrang, M. Ruat, E. Traiffort, J.C. Schwartz, J.M. Palacios, Three histamine receptors (H1, H2 and H3) visualized in the brain of human and non-human primates, Brain Res. 526 (1990) 322-327.

[15] H.L. Haas, O.A. Sergeeva, O. Selbach, Histamine in the nervous system, Physiol. Rev. 88 (2008) 1183-1241.

[16] A. Huber, G. Stuchbury, A. Burkle, J. Burnell, G. Munch, Neuroprotective Therapies for Alzheimers Disease, Curr. Pharm. Des. 12 (2006) 705-717.

[17] J. Li, X. Ma, Y. Wang, C. Chen, M. Hu, L. Wang, J. Fu, G. Shi, D. Zhang, T. Zhang, Methyl salicylate lactoside protects neurons ameliorating cognitive disorder through inhibiting amyloid beta-induced neuroinflammatory response in Alzheimer's disease, Front. Aging Neurosci. 10 (2018) 85.

[18] B. Feng, X. Li, J. Xia, S. Wu, Discovery of novel isoflavone derivatives as AChE/BuChE dual-targeted inhibitors: synthesis, biological evaluation and molecular modelling, J. Enzyme Inhib. Med. Chem. 32 (2017) 968-977.

[19] G. Wen, Q. Liu, H. Hu, D. Wang, S. Wu, Design, synthesis, biological evaluation, and molecular docking of novel flavones as H3 R inhibitors, Chem. Biol. Drug Des. 90 (2017) 580-589.

[20] R. Apodaca, C.A. Dvorak, W. Xiao, A.J. Barbier, J.D. Boggs, S.J. Wilson, T.W. Lovenberg, N.I. Carruthers, A New Class of Diamine-Based Human Histamine H3 Receptor Antagonists: 4-(Aminoalkoxy)benzylamines, J. Med. Chem. 46 (2003) 3938-3944**.**

[21] A.J. Barbier, C. Berridge, C. Dugovic, A.D. Laposky, S.J. Wilson, J. Boggs, L. Aluisio, B. Lord, C. Mazur, C.M. Pudiak, X. Langlois, W. Xiao, R. Apodaca, N.I. Carruthers, T.W. Lovenberg, Acute wake-promoting actions of JNJ-5207852, a novel, diamine-based H3 antagonist, Br. J. Pharmacol. 143 (2004) 649-661.

[22] K. Wingen, J.S. Schwed, K. Isensee, L. Weizel, A. Zivkovic, D. Odazic, H. Stark, Benzylpiperidine variations on histamine H3 receptor ligands for improved drug-likeness, Bioorg. Med. Chem. Lett. 24 (2014) 2236-2239.

[23] G.L. Ellman, K.D. Courtney, V. Andres, Jr., R.M. Feather-Stone, A new and rapid colorimetric determination of acetylcholinesterase activity, Biochem. Pharmacol. 7

(1961) 88-95.

[24] T. Jiang, Q. Sun, S. Chen, Oxidative stress: A major pathogenesis and potential therapeutic target of antioxidative agents in Parkinson's disease and Alzheimer's disease, Prog. Neurobiol. 147 (2016) 1-19.

[25] B. Tsoi, R.N. Yi, L.F. Cao, S.B. Li, R.R. Tan, M. Chen, X.X. Li, C. Wang, Y.F. Li, H. Kurihara, R.R. He, Comparing antioxidant capacity of purine alkaloids: a new, efficient trio for screening and discovering potential antioxidants in vitro and in vivo, Food Chem. 176 (2015) 411-419.

[26] A. Davalos, C. Gomez-Cordoves, B. Bartolome, Extending applicability of the oxygen radical absorbance capacity (ORAC-fluorescein) assay, J. Agric. Food Chem. 52 (2004) 48-54.

[27] G. Jonse, P. Willett, R.C. Glen, A.R. Leach, R. Taylor, Development and validation of a genetic algorithm for flexible docking, J. Mol. Biol. 267 (1997) 727-748.

[28] F.L. Heppner, R.M. Ransohoff, B. Becher, Immune attack: the role of inflammation in Alzheimer disease, Nat. Rev. Neurosci. 16 (2015) 358-372.

[29] M.T. Heneka, M.J. Carson, J. El Khoury, G.E. Landreth, F. Brosseron, D.L. Feinstein, A.H. Jacobs, T. Wyss-Coray, J. Vitorica, R.M. Ransohoff, K. Herrup, S.A. Frautschy, B. Finsen, G.C. Brown, A. Verkhratsky, K. Yamanaka, J. Koistinaho, E. Latz, A. Halle, G.C. Petzold, T. Town, D. Morgan, M.L. Shinohara, V.H. Perry, C. Holmes, N.G. Bazan, D.J. Brooks, S. Hunot, B. Joseph, N. Deigendesch, O. Garaschuk, E. Boddeke, C.A. Dinarello, J.C. Breitner, G.M. Cole, D.T. Golenbock, M.P. Kummer, Neuroinflammation in Alzheimer's disease, Lancet Neurol. 14 (2015) 388-405.

[30] C. Holmes, Review: systemic inflammation and Alzheimer's disease, Neuropathol. Appl. Neurobiol. 39 (2013) 51-68.

[31] C. Lu, Y. Guo, J. Yan, Z. Luo, H.B. Luo, M. Yan, L. Huang, X. Li, Design, synthesis, and evaluation of multitarget-directed resveratrol derivatives for the treatment of Alzheimer's disease, J. Med. Chem. 56 (2013) 5843-5859.

[32] Z. Sang, X. Qiang, Y. Li, R. Xu, Z. Cao, Q. Song, T. Wang, X. Zhang, H. Liu, Z.

Tan, Y. Deng, Design, synthesis and evaluation of scutellarein-O-acetamidoalkylbenzylamines as potential multifunctional agents for the treatment of Alzheimer's disease, Eur. J. Med. Chem. 135 (2017) 307-323.

[33] X. Lan, R. Liu, L. Sun, T. Zhang, G. Du, Methyl salicylate 2-O-beta-D-lactoside, a novel salicylic acid analogue, acts as an anti-inflammatory agent on microglia and astrocytes, J. Neuroinflammation 8 (2011) 98.

Highlights

- Compound **9b** was a satisfactory H3R/AChE inhibitor (IC_{50} = 0.27 μM for H_3R, IC_{50} = 0.081 μM for AChE).
- Compound **9b** possesses good neuroprotective effect against copper-induced SH-SY5Y -APPsw cell injury and potent anti-neuroinflammatory activity on BV-2.
- Compound **9b** displayed desirable pharmacokinetic properties, as well as good blood-brain barrier (BBB) permeability.
- Compound **9b** significantly improved cognitive dysfunction in scopolamine-induced AD mice.
- Compound **9b** was identified as a novel promising drug prototype candidate for the treatment of AD with innovative structural features and multifunctional profiles.